

Regio- and diastereo-selective formation of dicopper(I) and disilver(I) double helicates with chiral 6-substituted 2,2':6',2''-terpyridines

Gerhard Baum,^b Edwin C. Constable,^{*a} Dieter Fenske,^b Catherine E. Housecroft,^a Torsten Kulke,^a Markus Neuburger^a and Margareta Zehnder^a

^a Institut für Anorganische Chemie der Universität Basel, Spitalstrasse 51, 4056 Basel, Switzerland. E-mail: edwin.constable@unibas.ch

^b Institut für Anorganische Chemie der Universität Karlsruhe, Engesserstr., Geb.: 30 45, 76128 Karlsruhe, Germany

Received 19th November 1999, Accepted 21st January 2000

Two enantiomeric pairs of chiral terpy ligands (**I** and **II**; **III** and **IV**) bearing enantiopure bornyloxy substituents at the 6-position were prepared in high yield, stereoretentive reactions from (1*R*)-endo- or (1*S*)-endo-borneol; compounds **I**, **II** and **III** were structurally characterised. Dinuclear double helicates were formed upon reaction with copper(I) salts, but solvent-dependent and reversible formation of mononuclear or dinuclear double-helical complexes was observed with silver(I) salts. The double helicates are formed with good to excellent diastereo-selectivity for helical chirality. With these 6-substituted ligands, double helicates can exist as head-to-head (*HH*) or head-to-tail (*HT*) isomers; in solution, the *HT* isomers are favored, although solid state interactions can overcome this preference.

Metal-directed self-assembly is a powerful methodology in supramolecular chemistry and allows the specificity and transferability of self-assembly paradigms to be probed and quantified.^{1–4} Some of the best understood self-assembled motifs are based upon helical topographies^{5–8} and structural variation within helicands (*helical ligands*) allows the subtleties of metal–ligand coding to be investigated.^{9–12}

Helices are chiral, and the chirality is conveniently defined by the sense of rotation about a specific axis, leading to a *plus* (*P*) or *minus* (*M*) nomenclature (Fig. 1).¹³ Achiral ligands give a racemic mixture of enantiomeric *P* and *M* helices, although in exceptional cases, partial or complete spontaneous resolution may occur upon crystallisation.^{14,15} When chiral helicands are used, the presence of the additional chirality requires that the *P* and *M* helicates (*helical chelates*) are related as diastereomers and a range of examples have been reported in which one of the two is preferentially formed.^{13,16–32} Although helicates are usually prepared using commensurate ligand donor sets and metal ion acceptors (for example, two *N*₄-donor 2,2':6',2'':6'',2'''-quaterpyridine ligands and two four-coordinate tetrahedral metal centres), it is also possible to form helicates with incommensurate donor sets in which the coding is less precise. In particular, terpy forms double helicates with copper(I)^{31,33,34} and silver(I),^{32–35} although the latter complexes react readily with donor solvents such as MeCN to give mononuclear

species.^{32,35} Initial studies showed that chiral substituents at the 4'-position of terpy ligands were ineffective in chiral induction (*i.e.* no significant diastereomeric excesses)^{36,37} and we subsequently embarked upon the synthesis of terpy ligands in which the centres of chirality would lie closer to the metal centres in their complexes. In this paper we describe regio-selective and diastereoselective formation of copper(I) and silver(I) helicates with terpy ligands bearing chiral substituents in the 6-position and also show a solvent-dependent inter-conversion of mononuclear and dinuclear double-helical silver(I) complexes. Some of these results have previously appeared in communication form.^{31,32}

Results and discussion

Terpy helicates and ligand design

Usually terpy ligands behave as tridentate *N*₃ donors, although mono- and di-dentate bonding modes are now well-established.³⁸ It is also known that terpy and other *N*₃ donor ligands form dinuclear double helicates with copper(I) and silver(I)^{5–8} in which the six donor atoms are incommensurate with the four-coordinate, near-tetrahedral geometries commonly associated with these ions. The precise bonding arrangements are somewhat variable and depend upon the exact structure of the helicand, but limiting cases involving two two-coordinate metal centres (A), two three-coordinate metal centres (B), “bridging” pyridine donors (C) or one two-coordinate and one four-coordinate metal centre (D) are known (Fig. 2). In the case of dicopper(I) helicates, aryl substituents in the 6- and 6''-positions have been shown to stabilise the system with respect to oxidation to mononuclear copper(II) complexes whilst they have no significant effect on the silver(I) species.^{33–35}

The new terpy ligands were designed to investigate a number of factors in helicate formation; (i) a chiral substituent was introduced in the 6-position to maximise the proximity to the metal ion to see whether diastereoselective formation of *P* or *M* helicates could be achieved, (ii) we were interested whether it

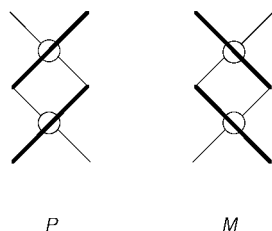
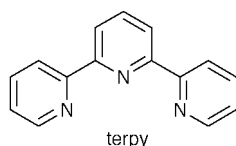


Fig. 1 Enantiomeric *P* and *M* dinuclear double helicates. If the ligand is achiral, a racemate containing equal amounts of the two enantiomeric helicates is expected.



was essential to have aryl substituents in the 6- and 6''-positions to stabilise dicopper(I) double helicates and (iii) we were interested in using ligands in which the 6- and 6''-positions bore

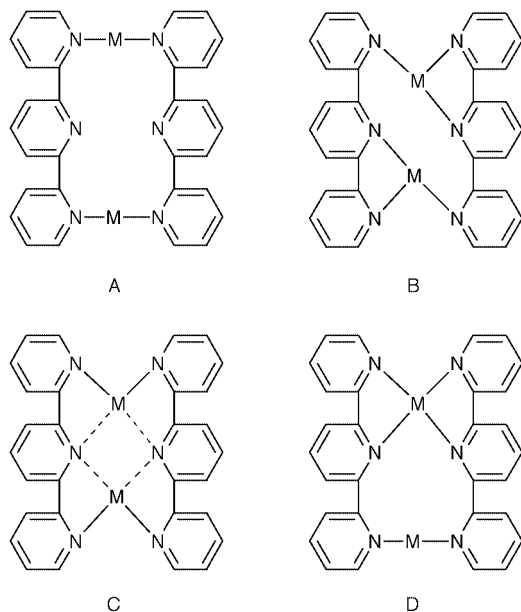


Fig. 2 Representations of the possible metal ligand interactions in incommensurate dinuclear double helicates derived from terpy ligands with silver(I) or copper(I). The structures are represented in the flattened topographic form.

different substituents and could give rise to head-to-head (*HH*) or head-to-tail (*HT*) directional isomers (Fig. 3).^{39–41} We prefer the term directional isomerism for describing *HH* or *HT* isomers although they are rigorously described as structural isomers. As indicated in Fig. 3, a total of eight isomers is possible if only ligand-homochiral systems (*i.e.* those in which the chiral substituents of the two ligands possess the same absolute configuration) are considered and the directional consequences of structure D in which the metal centres are inequivalent are disregarded. The eight isomers are partitioned into sets of *HH* and *HT* isomers; within each set, there is a pair of *P* or *M* helicates for the (*R;R*) and (*S;S*) combinations. Within the *HH* and *HT* subsets, the *M*-(*R;R*) and *P*-(*S;S*) compounds are enantiomers, as is the *P*-(*R;R*) and *M*-(*S;S*) pair; furthermore, within the *HH* and *HT* subsets, all other combinations of compounds are related as diastereomers. The *HH* and *HT* compounds are, of course, structural or directional isomers. Inclusion of the ligand-heterochiral (*R;S*) complexes generates an additional four isomers, which will not be discussed in detail in this paper.

The use of *C*₁ symmetrical ligands allows us to probe selectivity for *HH* or *HT* helicate formation in self assembly, in contrast to earlier studies using *C*₂ symmetrical ligands predisposed towards *HH* helicate formation.¹⁷ Although we had spectroscopic evidence that terpy ligands gave solution disilver(I) double helicates, no such species had been characterised and we hoped that chiral ligands would additionally allow the solvent-dependent interconversion between mononuclear and dinuclear silver(I) complexes to be investigated.

For synthetic versatility we used [(1*S*)-endo]-(-)- and [(1*R*)-endo]-(+)-borneol, which are readily commercially available in high enantiomeric purity, to generate the chiral auxiliary groups of the ligands. Although bornyloxy substituents are probably not as effective at chiral induction as fused pineno groups^{13,20} they are readily and cheaply available in both antipodes from the chiral pool. A suite of four ligands consisting of two pairs of enantiomers (1*S*)-**I** and (1*R*)-**II** (generically *L*¹), and (1*S*)-**III** and (1*R*)-**IV** (generically *L*²), was chosen.

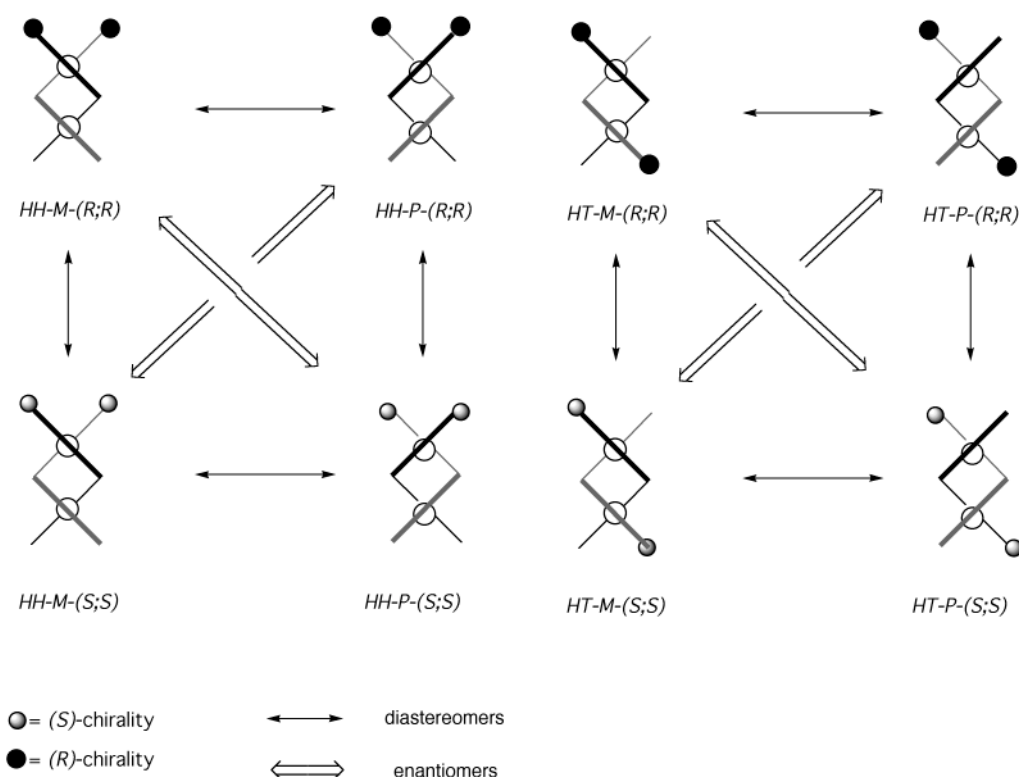
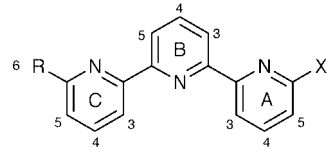


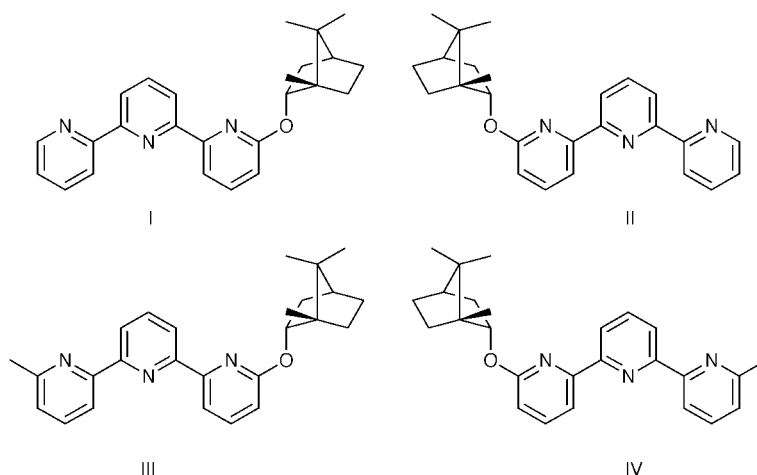
Fig. 3 The introduction of substituents at one end of a helicand can lead to head-to-head *HH* and head-to-tail *HT* directional isomers. If the substituents are chiral, then sets of directional *HH* and *HT* isomers are obtained consisting of enantiomeric pairs of compounds {*P*-(*R;R*) and *M*-(*S;S*)} and {*P*-(*S;S*) and *M*-(*R;R*)} double helicates are obtained.

Table 1 250 MHz ^1H NMR spectroscopic data for the aromatic and methyl substituent (where appropriate) resonances of the ligands, **I**, **III**, **IV** and **X** and the copper(i) and silver(i) complexes of **I** and **III**. The spectra of **II** and **IV** and their complexes are identical to those of their enantiomers within experimental error



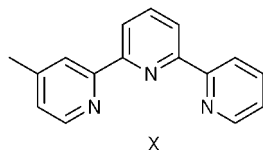
| | 3A | 4A | 5A | 3B | 4B | 5B | 3C | 4C | 5C | 6C | Me |
|----------------------------|------|------|------|--------------|--------------|--------------|------|------|------|------|------|
| I/II ^a | 8.18 | 7.70 | 6.78 | 8.35 | 7.92 | 8.41 | 8.61 | 7.83 | 7.30 | 8.68 | — |
| III/IV ^a | 8.19 | 7.70 | 6.78 | 8.34 | 7.91 | 8.37 | 8.44 | 7.72 | 7.17 | — | 2.62 |
| VI ^a | 8.58 | 7.68 | 7.49 | 8.42 | 7.92 | 8.38 | 8.48 | 7.72 | 7.18 | — | 2.68 |
| X ^a | 8.39 | 7.71 | 7.17 | 8.42 | 7.92 | 8.46 | 8.61 | 7.83 | 7.30 | 8.68 | 2.63 |
| 1/2 ^{b,f} | 7.59 | 7.26 | 6.57 | 8.02–8.16 | 8.02–8.16 | 8.02–8.16 | 7.96 | 7.78 | 7.29 | — | 2.19 |
| 3/4 ^b | 7.96 | 7.91 | 6.89 | 8.19 | 8.15 | 8.32 | 8.21 | 7.94 | 7.39 | 8.39 | — |
| 7/8 ^c | 8.04 | 7.99 | 6.81 | 8.21 | 8.29 | 8.44 | 8.15 | 7.97 | 7.20 | 7.87 | — |
| 5/6 ^{b,f} | 7.86 | 7.78 | 6.80 | ^d | ^d | ^d | 7.98 | 7.88 | 7.29 | — | 2.31 |
| 9/10 ^e | 7.97 | 7.87 | 6.81 | 8.26 | 8.26 | 8.37 | 7.97 | 7.87 | 7.27 | — | 2.13 |

^a CDCl_3 . ^b CD_3CN . ^c CD_3OD . ^d ABC system, δ 8.14–8.29. ^e 91.5% CD_3OD /8.5% CD_3CN . ^f Major diastereomer.



The chiral terpy ligands I–IV

Synthesis. The preparation of the ligands L^1 utilises the known 6-bromo compound **V**⁴² but for L^2 , the new compound **VI** was required. The reaction of 2-acetyl-6-methylpyridine **VII**^{43,44} with I_2 in pyridine gave the Kröhnke⁴⁵ salt **VIII**, which was isolated in 96% yield as a 1:1 mixture with pyridinium iodide (^1H NMR assay). This crude mixture was reacted with the Mannich salt **IX**^{46,47} in the presence of $[\text{NH}_4][\text{OAc}]$ to give the bromo compound **VI** in 55% yield. The alkoxides of [(1*S*)-endo]-(-)- or [(1*R*)-endo]-(+)-borneol were reacted with half an equivalent of **V** or **VI** (Scheme 1) to give the new ligands as microanalytically pure white solids after recrystallisation from MeOH. The yields of L^1 were acceptable (70–75%) but those of L^2 were consistently lower ($\approx 50\%$). In each case, significant amounts (up to 30%) of the reduction products terpy (from **V**) and 6-methyl-2,2':6',2''-terpyridine **X** (from **VI**) were obtained.



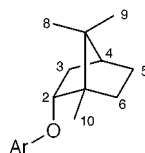
The time-of-flight (TOF) mass spectra showed, in each case, molecular ion peaks together with daughter peaks corresponding to the loss of bornyl groups. The ^1H NMR spectra (Tables 1 and 2) were fully assigned by chemical shift comparison, COSY and NOESY difference spectroscopy and the chemical shifts of

enantiomeric ligands were identical within experimental error. A comparison of 6- and 4'-bornyloxy substituted ligands^{36,37} reveals significant shift differences for the $\text{H}^{2\text{exo}}$ resonance of the chiral auxiliary, indicating that our design strategy was successfully changing the interactions between the metal-binding terpy domain and the chiral substituent.

Optical rotations (Na-D line, Table 3) and CD spectra of enantiomers were equal and opposite with the ligands possessing an enantiomeric purity better than the starting borneols; in each case, the sign of the rotation in the terpy derivative is the same as that of the starting borneol. The CD spectra have maximum signal intensities of the order of $\Delta\epsilon \pm 2.5 \text{ M}^{-1} \text{ cm}^{-1}$ and show two absorptions of the same sign at $\approx 265 \text{ nm}$ and $\approx 298 \text{ nm}$ corresponding to $\pi^* \leftarrow n$ and $\pi^* \leftarrow \pi$ transitions in the absorption spectrum. The presence of the 6-methyl substituent in L^2 does not significantly change the chiroptical properties.

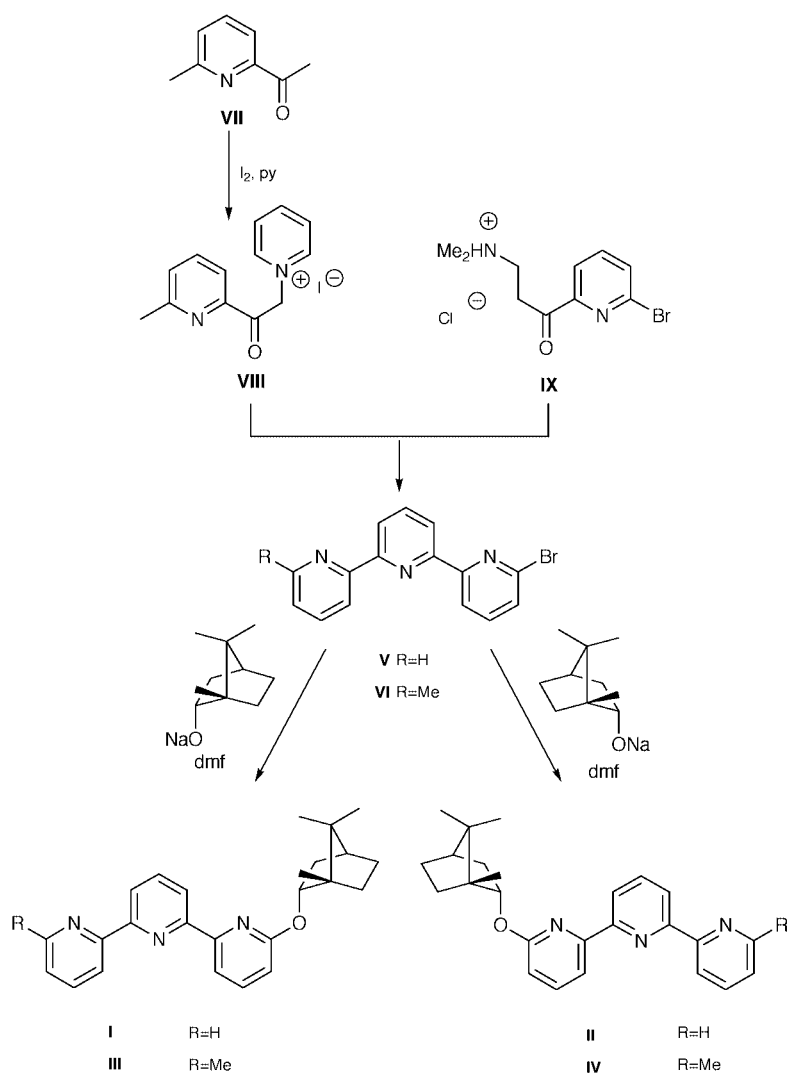
Structural studies. Compounds **I**, **II** and **III** were structurally characterised. Parameters for compounds **I** and **II** only differed within experimental error. Fig. 4a shows the structure of the pair of crystallographically independent molecules of **I** present in the lattice; all intramolecular distances and angles are normal. Each terpy domain is partitioned into a near-planar bpy region comprising the central ring and the unsubstituted terminal ring (least squares planes 5.42, 6.64°) and the substituted ring (least squares planes with the central ring, 13.66, 14.37°). The bpy domains of adjacent molecules are π -stacked (Fig. 4b) with interplanar angles 3.69 and 8.45°; intradimer

Table 2 250 MHz ^1H NMR spectroscopic data for the aliphatic resonances of the ligands **I** and **III** and their copper(I) and silver(I) complexes. The spectra of **II** and **IV** and their complexes are identical to those of their enantiomers within experimental error



| | H | 2 | 3 | 4 | 5 | 6 | 8 | 9 | 10 |
|----------------------------|-------------|------|-----------|------|-----------|-----------|------|------|------|
| I/II ^a | <i>exo</i> | 5.22 | 2.56–2.69 | 1.74 | 1.73–1.89 | 2.18–2.30 | 0.94 | 1.06 | 0.96 |
| | <i>endo</i> | | 1.15 | | 1.25–1.40 | 1.30–1.45 | | | |
| III/IV ^a | <i>exo</i> | 5.25 | 2.57–2.70 | 1.74 | 1.73–1.88 | 2.18–2.30 | 0.94 | 1.06 | 0.96 |
| | <i>endo</i> | | 1.15 | | 1.24–1.38 | 1.30–1.45 | | | |
| 1/2 ^{b,f} | <i>exo</i> | 4.79 | 2.32–2.46 | 1.65 | 1.62–1.76 | 1.82–1.96 | 0.86 | 0.87 | 0.78 |
| | <i>endo</i> | | 0.87 | | 1.06–1.20 | 1.16–1.30 | | | |
| 3/4 ^b | <i>exo</i> | 4.58 | 2.38–2.52 | 1.70 | 1.58–1.72 | 1.94–2.08 | 0.88 | 0.96 | 0.75 |
| | <i>endo</i> | | 0.93 | | 0.96–1.10 | 1.04–1.18 | | | |
| 6/7 ^c | <i>exo</i> | 4.27 | 2.20–2.34 | 1.54 | 1.31–1.45 | 1.20–1.34 | 0.65 | 0.78 | 0.41 |
| | <i>endo</i> | | 0.61 | | 0.60–0.74 | 0.57–0.71 | | | |
| 5 ^{b,f} | <i>exo</i> | 4.62 | 2.32–2.46 | 1.63 | 1.52–1.66 | 1.74–1.88 | 0.80 | 0.87 | 0.68 |
| | <i>endo</i> | | 0.83 | | 0.90–1.04 | 1.00–1.14 | | | |
| 8/9 ^{d,e} | <i>exo</i> | 4.44 | 2.26–2.40 | 1.58 | 1.40–1.54 | 0.71 | 0.94 | 0.82 | 0.53 |
| | <i>endo</i> | | 0.70 | | 0.70–0.84 | 0.78–0.92 | | | |

^a CDCl_3 . ^b CD_3CN . ^c CD_3OD . ^d ABC system, δ 8.14–8.29. ^e 91.5% CD_3OD /8.5% CD_3CN . ^f Major diastereomer.



Scheme 1

centroid to centroid distances (central–central', 4.003 Å, outer–outer', 3.981 Å) are slightly longer than the interdimer contacts (central–central', 3.879 Å, outer–outer', 3.842 Å).

In compound **III**, the lattice also contains a dimer (Fig. 5a) and, once again, exhibits a near-planar bpy region (central ring and methyl-substituted ring, least squares planes 1.72, 3.56°);

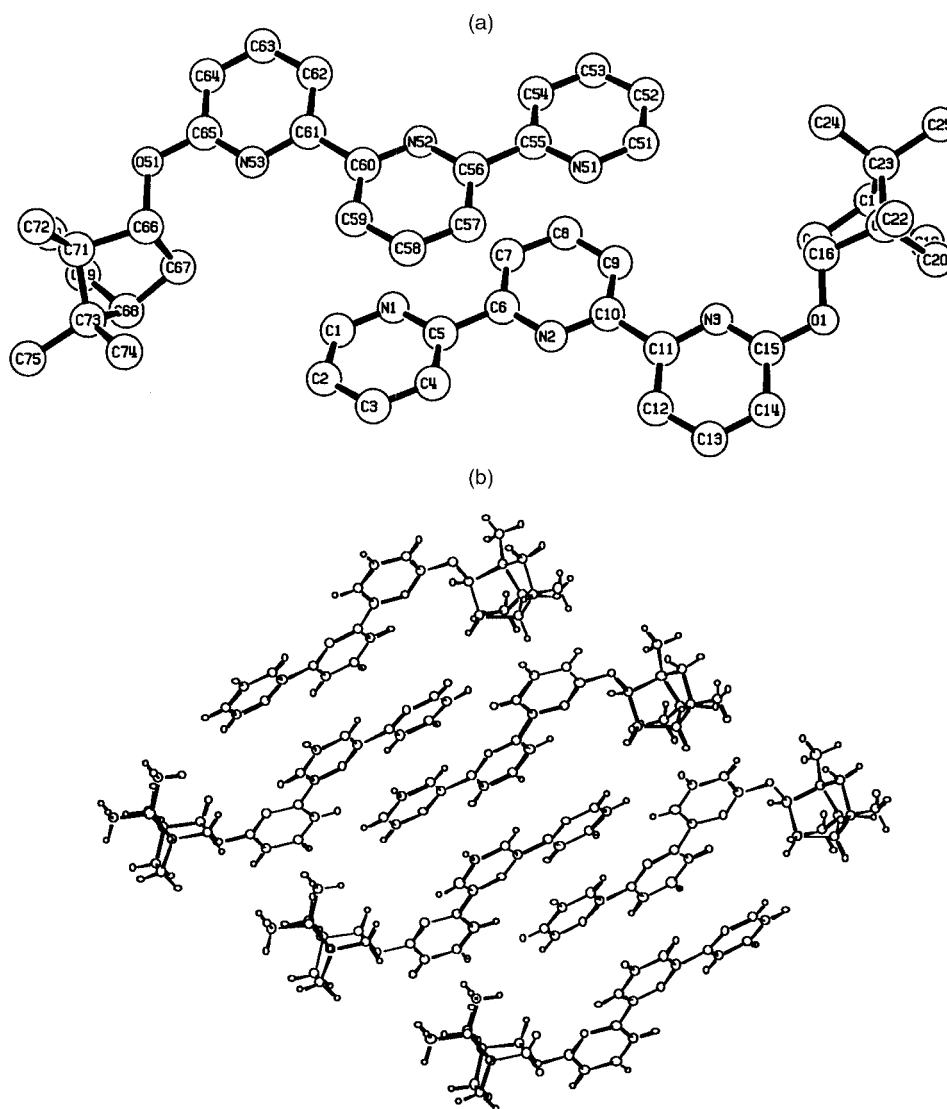


Fig. 4 Crystal and molecular structure of (a) the pair of crystallographically non-equivalent chiral ligands **I** showing the numbering scheme; H atoms omitted for clarity and (b) the crystal packing showing the extended π -stacking that is present.

the third ring with the chiral substituent is now more skewed (least squares planes with the central ring, 19.88, 22.97°) to minimise interactions with the methyl substituent of the other molecule in the dimer. The methyl groups also prevent extended π -stacking (Fig. 5b) and although the two molecules within the dimer are stacked (intradimer centroid-to-centroid distances 3.800 Å), no longer range interactions are observed. Selected bond lengths and bond angles are presented in Table 4 and material relating to the data collection and structure solution in Table 5. The data sets for the compounds **I**, **II** and **III**, which contain no atoms heavier than oxygen were not of high enough quality to unambiguously assign the absolute configurations on the basis of the Flack parameters. However, the synthetic method is unambiguous and the absolute configurations follow from the borneol used.

Synthesis and properties of copper complexes

Synthesis. Reaction of L^1 or L^2 with $[\text{Cu}(\text{MeCN})_4][\text{PF}_6]$ in degassed MeCN or MeOH gave orange-red solutions from which crude complexes were obtained after removal of the solvent. Although complexes with both sets of ligands could be obtained, those with L^1 were significantly air sensitive. Recrystallisation by diffusion of diethyl ether into MeCN or MeOH solutions gave thin orange crystals of $[\text{Cu}_2(L^2)_2][\text{PF}_6]_2$ in overall 72–78% yield, whereas $[\text{Cu}_2(L^1)_2][\text{PF}_6]_2$ rapidly oxidised to green copper(II) complexes under the same conditions. The

$[\text{Cu}_2(L^1)_2][\text{PF}_6]_2$ complexes were not further investigated. The complexes $[\text{Cu}_2(L^2)_2][\text{PF}_6]_2$ **1** and **2** (with **III** and **IV** respectively) were fully characterised and partial elemental analysis confirmed the expected ligand:copper ratio of 1:1; they are stable as solids, but somewhat air-sensitive over prolonged periods in solution. Time-of-flight mass spectrometric data suggested the formulation $[\text{Cu}_2(L^2)_2][\text{PF}_6]_2$ and as previously established^{33,34} the 2:2 stoichiometry is only compatible with a double-helical structure. The 6-methyl substitution appears to stabilise the copper(I) state and retard oxidation to mononuclear copper(II) species. However, complexes with L^2 are subjectively not as stable as those with ligands bearing 6,6'-diphenyl substituents, whose dicopper(I) species are completely air-stable.

Spectroscopic studies. The ^1H NMR spectra of CD_3CN solutions of crude **1** and **2** before recrystallisation were identical and showed two solution species in a ratio of 13:2. Data for the major compound are presented in Tables 1 and 2. The observation of two solution species could have three origins (i) mononuclear $[\text{Cu}(L^2)(\text{MeCN})]^+$ and dinuclear $[\text{Cu}_2(L^2)_2]^{2+}$ species (ii) diastereomeric *P* and *M* helicates or (iii) *HH* and *HT* isomers. The resonances of the major solution species are slightly broadened in the aromatic region, whereas those of the bornyl-oxy substituent are sharp. This broadening is assigned to a dynamic process in which the metal scrambles between some or all of the modes in Fig. 2.^{33,34} We can eliminate possibility (i) for

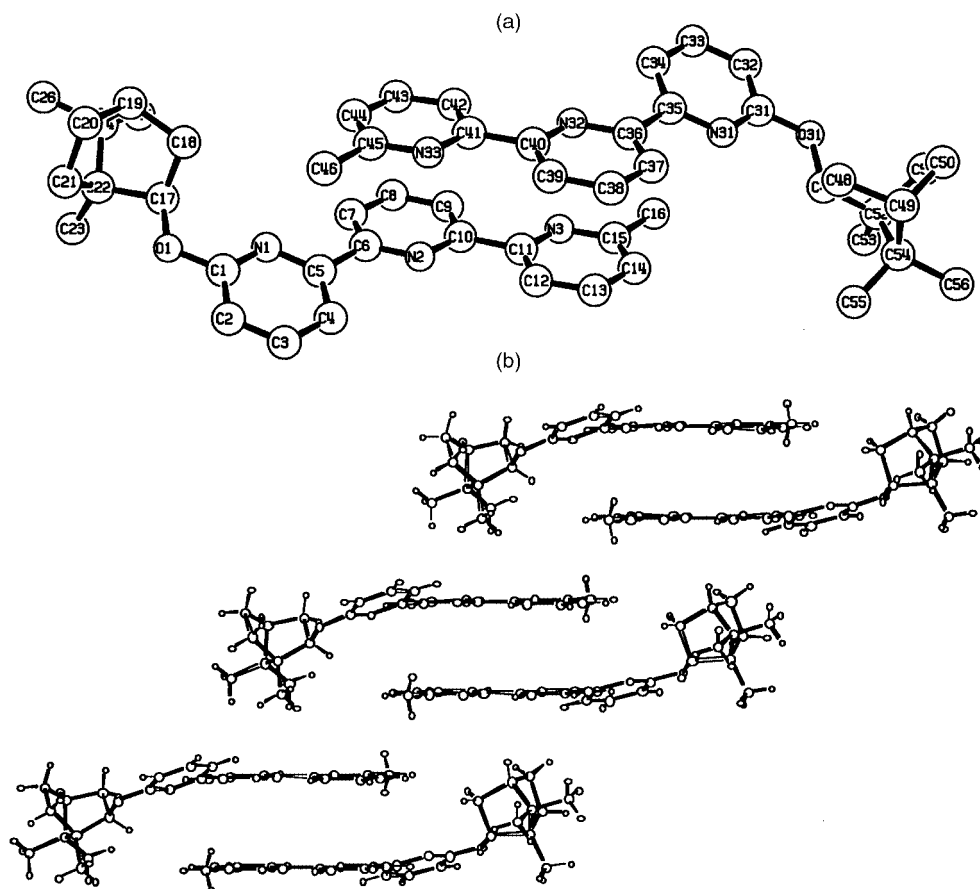


Fig. 5 Crystal and molecular structure of (a) the pair of crystallographically non-equivalent chiral ligands **III** showing the numbering scheme; H atoms omitted for clarity and (b) the crystal packing showing the effect of the 6-methyl substituent in preventing extended π -stacking in the lattice.

Table 3 Compilation of the free ligand and complex rotational values and CD signal intensities. The $[\alpha]_D$ and $[M]_D$ values come from polarimetric measurements at 23 °C and the $\Delta\epsilon$ values from CD spectroscopy

| | $[\alpha]_D/\text{deg g}^{-1}\text{cm}^3\text{dm}^{-1}$ | $[M]_D^a/\text{deg cm}^3\text{dm}^{-1}\text{mol}^{-1}$ | $\Delta\epsilon_{\text{max}}/\text{M}^{-1}\text{cm}^{-1}$ |
|--------------------------|---|--|--|
| I ^b | −62.6 | −241 | $\Delta\epsilon_{264}$ −1.6 $\Delta\epsilon_{299}$ −1.5 |
| II ^b | +62.7 | +242 | $\Delta\epsilon_{264}$ +1.5 $\Delta\epsilon_{299}$ +1.7 |
| III ^b | −62.1 | −248 | $\Delta\epsilon_{265}$ −2.0 $\Delta\epsilon_{296}$ −2.3 |
| IV ^b | +62.3 | +249 | $\Delta\epsilon_{265}$ +2.0 $\Delta\epsilon_{296}$ +2.2 |
| <i>M-1</i> ^c | ^d | ^d | $\Delta\epsilon_{219}$ −15 $\Delta\epsilon_{312}$ −8 |
| <i>P-2</i> ^c | ^d | ^d | $\Delta\epsilon_{219}$ +17 $\Delta\epsilon_{312}$ +8 |
| <i>M-7</i> ^e | −203.8 ^[a] | −2602 | $\Delta\epsilon_{214}$ −22.2 $\Delta\epsilon_{329}$ −19.7 |
| 3 ^c | −62.6 ^[b] | −640 | $\Delta\epsilon_{328}$ −1.9 |
| <i>P-8</i> ^c | +199.9 ^[b] | +2541 | $\Delta\epsilon_{214}$ +24.0 $\Delta\epsilon_{329}$ +20.2 |
| 4 ^c | +60.6 | +620 | $\Delta\epsilon_{214}$ −44.5 $\Delta\epsilon_{293}$ +4.7 |
| <i>M-9</i> ^e | −238.4 | −1506 | $\Delta\epsilon_{332}$ −35.8 $\Delta\epsilon_{218}$ −2.0 |
| 5 ^c | −64.4 | −640 | $\Delta\epsilon_{325}$ −1.5 $\Delta\epsilon_{214}$ +44.5 |
| <i>P-10</i> ^e | +236.1 | +3080 | $\Delta\epsilon_{293}$ −3.8 $\Delta\epsilon_{332}$ +36.3 |
| 6 ^c | +65.2 | +620 | |

^a $[M]_D = [\alpha]_D \times \text{MW}/100$. ^b CDCl_3 solution. ^c MeCN solution. ^d Solutions too highly coloured to determine $[\alpha]_D$ reliably. ^e MeOH solution.

the minor solution species because (a) the subspectrum exhibits the same line broadening and (b) shows shift differences too small to correspond to formation of a mononuclear complex.³⁵ Because the shift differences between the solution species are small, it is most likely that the minor component arises from a helicate with opposite helical chirality rather than *HH/HT* isomerism, for which substantial shift differences are expected.^{39–41} Molecular modelling studies using parameters derived from structurally characterised double helicates with 2,2':6',2''-terpyridines^{33,34} indicated that the *HH* isomers would be of significantly higher energy than the *HT* isomers and that enantiomeric *HT-M-1* and *HT-P-2* helicates should be stabilised with respect to the diastereomeric *HT-P-1* and *HT-M-2* species by about 10 kJ mol^{−1}. Assuming this analysis to be correct, the ¹H NMR data indicate the formation of *HT-M-1* and *HT-P-2* helicates respectively with a diastereomeric excess (DE) of 75%.

Recrystallisation of the crude complexes **1** or **2** gave good quality crystals of compounds containing only the major isomer as established by ¹H NMR spectroscopy of freshly prepared solutions. Solutions of these crystals did not regenerate the minor compound within a 2–3 h period, indicating that interconversion of the diastereomeric helicates is slow, in contrast to related double-helical complexes with 2,2':6',2''-quaterpyridines.¹³ The unequivocal confirmation of stereochemistry came from solid state structural determinations of the salts **1**·2MeCN and **2**·2MeCN.

Solid state structures of $[\text{Cu}_2(\text{L}^2)_2][\text{PF}_6]_2 \cdot 2\text{MeCN}$. Both structures were solved in the non-centrosymmetric space group *P2*₁*2*₁*2* and were identical within experimental error.³¹ The double-helical geometry was confirmed and the determination showed that the major diastereomer of the cation in **1** exhibits *M* helical chirality, whilst that of **2** adopts a *P* conformation.

Table 4 Selected bond lengths (Å) and angles (°) for compounds **I**, **III** and **10** with e.s.d.s in parentheses

| I | | III | | 10 | |
|------------------|----------|------------------|----------|--------------|------------|
| N(1)–C(1) | 1.339(5) | O(1)–C(1) | 1.361(3) | Ag–N(1) | 2.154(3) |
| N(1)–C(5) | 1.335(4) | O(1)–C(17) | 1.449(3) | Ag–Ag | 2.9387(11) |
| C(5)–C(6) | 1.490(4) | N(1)–C(1) | 1.314(3) | Ag–N(2) | 2.6165(19) |
| N(2)–C(6) | 1.336(4) | N(1)–C(5) | 1.352(3) | Ag–N(3) | 2.166(3) |
| N(2)–C(10) | 1.339(4) | C(5)–C(6) | 1.493(4) | | |
| C(10)–C(11) | 1.486(4) | N(2)–C(6) | 1.338(3) | | |
| N(3)–C(11) | 1.347(4) | N(2)–C(10) | 1.343(3) | | |
| N(3)–C(15) | 1.311(4) | C(10)–C(11) | 1.496(4) | | |
| C(15)–O(1) | 1.357(4) | N(3)–C(11) | 1.337(3) | | |
| O(1)–C(16) | 1.442(4) | N(3)–C(15) | 1.341(4) | | |
| | | C(15)–C(16) | 1.503(5) | | |
| C(1)–N(1)–C(5) | 117.4(3) | C(1)–O(1)–C(17) | 116.9(2) | N(1)–Ag–Ag | 91.33(6) |
| C(6)–N(2)–C(10) | 118.9(3) | C(1)–N(1)–C(5) | 117.5(2) | N(1)–Ag–N(2) | 114.59(8) |
| C(11)–N(3)–C(15) | 117.7(3) | C(6)–N(2)–C(10) | 117.8(2) | N(1)–Ag–N(3) | 172.75(7) |
| C(15)–O(1)–C(16) | 116.5(2) | C(11)–N(3)–C(15) | 118.4(3) | Ag–Ag–N(2) | 57.15(4) |
| | | | | Ag–Ag–N(3) | 91.96(5) |
| | | | | N(2)–Ag–N(3) | 72.58(8) |

Table 5 Summary of crystallographic data for **I**, **II**, **III** and **10**

| | I ^a | II | III ^a | 10 ^b |
|---|--|--|--|--|
| Molecular formula | C ₂₅ H ₂₇ N ₃ O | C ₂₅ H ₂₇ N ₃ O | C ₂₆ H ₂₉ N ₃ O | C ₅₂ H ₅₈ Ag ₂ F ₁₂ N ₆ O ₂ P ₂ |
| <i>M</i> | 385.51 | 385.51 | 399.54 | 1304.72 |
| Colour, habit | Colourless cube | Colourless needle | Colourless cube | Colourless block |
| Crystal system | Monoclinic | Monoclinic | Monoclinic | Monoclinic |
| Space group | <i>P</i> 2 ₁ | <i>P</i> 2 ₁ | <i>P</i> 2 ₁ | <i>C</i> 2 |
| <i>a</i> /Å | 13.177(2) | 13.190(2) | 6.292(2) | 24.641(7) |
| <i>b</i> /Å | 7.744(1) | 7.750(1) | 10.696(1) | 12.669(2) |
| <i>c</i> /Å | 21.471(2) | 21.469(1) | 29.978(4) | 8.390(3) |
| β /° | 105.38(1) | 105.390(7) | 92.81(1) | 95.59(3) |
| <i>V</i> /Å ³ | 2112.6(4) | 2116.1(4) | 2219.0(6) | 2606.7(13) |
| <i>Z</i> | 4 | 4 | 4 | 2 |
| <i>D</i> _c /g cm ^{−3} | 1.21 | 1.21 | 1.20 | 1.662 |
| <i>T</i> /K | 293 | 293 | 293 | 203 |
| <i>F</i> (000) | 824 | 824 | 856 | 1320 |
| μ /mm ^{−1} | 0.55 | 0.55 | 0.54 | 0.903 |
| θ range/° | 2.2–74.3 | 2.2–74.3 | 2.2–74.3 | 3.99–28.08 |
| No. reflections measured | 4199 | 4274 | 4404 | 4821 |
| No. reflections observed | 3458 | 3496 | 3837 | 4773 |
| | <i>I</i> > 2 σ [<i>I</i>] | <i>I</i> > 3 σ [<i>I</i>] | <i>I</i> > 2 σ [<i>I</i>] | <i>I</i> > 2 σ [<i>I</i>] |
| No. parameters | 525 | 524 | 542 | 376 |
| No. restraints | 0 | 0 | 0 | 1 |
| <i>R</i> | 0.0651 | 0.0544 | 0.0469 | 0.0253 |
| <i>wR</i> | 0.0786 | 0.0652 | 0.0552 | 0.0687 |
| Largest difference peak, hole/e Å ^{−3} | 0.27, −0.32 | 0.33, −0.31 | 0.34, −0.20 | 0.52, −0.47 |

^a Enraf-Nonius CAD4 diffractometer, graphite monochromated Cu-K α radiation. ^b Stoe IPDS image plate diffractometer, graphite monochromated Mo-K α radiation.

The Flack parameters⁴⁸ are close to zero, establishing the absolute structures and confirming the assignment on the basis of the (known) configuration of the bornyl groups. In each case the *HT* isomer is found in the solid state. The solid state molecular structure of the [Cu₂(**III**)₂]²⁺ cation in **1** is presented in Fig. 6a and 6b. The Cu...Cu distance is 2.688(1) Å, which is significantly longer than in related complexes^{5–8} (2.570–2.631 Å) and represents an increase in helical pitch arising from steric repulsion between the substituents. The two copper centres are equivalent and best described as two coordinate with a *trans* N–Cu–N angle of 165.2(1)° and typical Cu–N bond distances (1.947(3) Å, 1.940(3) Å); each copper exhibits longer contacts to the central pyridine ring N atoms (2.431(2) Å, 2.317(3) Å) and the central pyridine rings may be regarded as semi-bridging *N*-donors. The helical twist arises from successive, approximately constant, interannular torsions between the pyridine rings (28.3°, 29.5°).

Chiroptical properties. The CD curves of the recrystallised, major diastereomers of **1** and **2** (MeCN, *c* ≤ 1.0 × 10^{−4} M) are equal and opposite within experimental error and a number

of features are evident. Firstly, the CD activity ($\Delta\epsilon_{312} \pm 8$ M^{−1} cm^{−1}) is small in comparison to, but resembles that of, qtpy helicates.¹³ A further response is found in the visible region (440 nm) indicating some perturbation of metal-centered orbitals occurs; the relatively low CD activity seems to be a feature of tridentate ligands as a related 2,6-bis(oxazolinepyridine)silver(i) complex also showed small $\Delta\epsilon$ values (10.15 M^{−1} cm^{−1}).⁴⁹ The sign of the 312 nm CD response gives the helical screw sense⁵⁰ and *M*-**1** and *P*-**2** structures are assigned to the dominant solution species in agreement with the solid state structures.

Synthesis and properties of silver complexes

Synthesis. Reaction of the ligands with AgOAc in MeOH gave colourless solutions from which PF₆[−] complexes were precipitated in near-quantitative yield. The crude complexes were recrystallised by diffusing diethyl ether into MeOH, MeNO₂ or MeCN solutions. With **L**¹, the crystals obtained from MeCN were qualitatively and quantitatively different from those from MeOH or MeNO₂. The complexes [Ag₂(**L**¹)₂][PF₆]₂ and

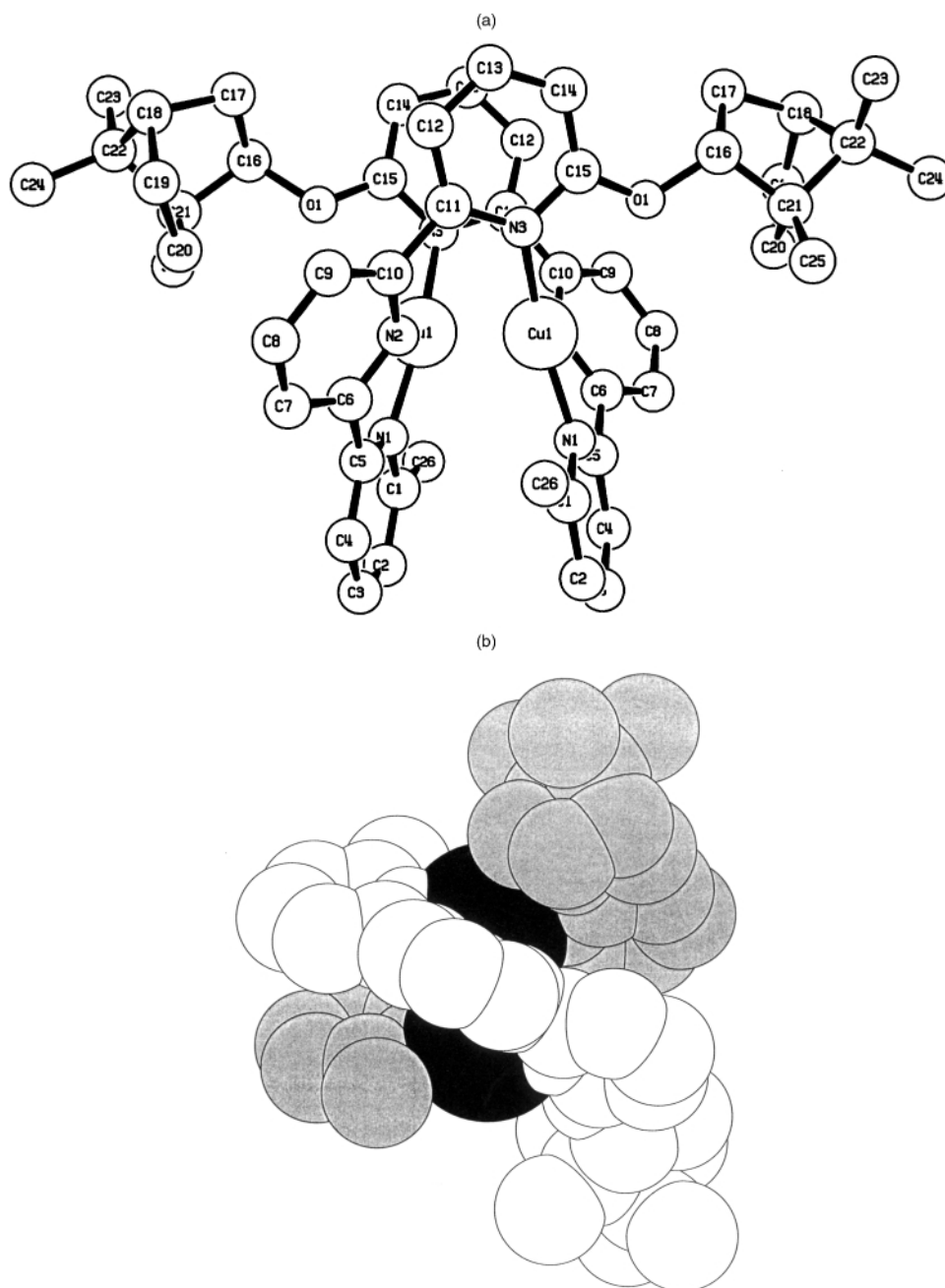


Fig. 6 Crystal and molecular structure of (a) the *HT* double-helical cation in the lattice of *M*·1.2MeCN showing the numbering scheme; H atoms omitted for clarity and (b) a space-filling representation emphasising the *M*-helicity.

$[\text{Ag}_2(\text{L}^2)_2][\text{PF}_6]_2$ were obtained from MeOH or MeNO₂ solution and were fully characterised; they are soluble in chlorinated solvents and were single compounds according to TLC analysis. The compounds are photosensitive both in the solid state and in solution, and crystals exposed to direct sunlight form a brown coating within hours, whilst solutions turn yellow then brown. The ES mass spectra of solutions in MeOH or Me₂CO of the solids obtained from MeNO₂ displayed variable ratios of $\{\text{Ag}(\text{L})\}^+$, $\{\text{Ag}(\text{L})_2\}^+$ and $\{\text{Ag}_2(\text{L})_2(\text{PF}_6)\}^+$ species, whereas MeCN solutions showed predominantly $\{\text{Ag}(\text{L})\}^+$ complexes and at concentrations $<10^{-5}$ M, no $\{\text{Ag}_2(\text{L})_2(\text{PF}_6)\}^+$ peaks were observed. This suggests the presence of $[\text{Ag}_2(\text{L})_2]^{2+}$ species in less-coordinating solvents and an equilibrium between $[\text{Ag}_2(\text{L})_2]^{2+}$ and $[\text{Ag}(\text{L})(\text{MeCN})]^+$ in MeCN. In previous studies, we have isolated only $[\text{Ag}(\text{L})(\text{MeCN})]^+$ species from MeCN solutions.³⁵ When samples of the *L*¹ complexes were recrystallised from MeCN, compounds were obtained which exhibited characteristic nitrile absorptions in their IR spectra (2305 and 2273 cm⁻¹) although the analogous *L*² complexes did not.

When a compressed KBr disc of the complex with **II** was stored for 2 h at 80 °C and 65 Torr, the nitrile signals diminished in intensity and had disappeared after 12 h. The MeCN complex persists in the solid state with *L*¹, but the situation is less clear with *L*². The facile loss of MeCN meant that attempts to dry samples for microanalysis gave compounds which analyzed as $\{\text{Ag}(\text{L}^1)(\text{PF}_6)\}_n$.

Spectroscopic studies. The ¹H NMR data for solutions of the complexes are given in Tables 1 and 2: the spectra of solutions in CD₃OD of the crude, unrecrystallised compounds obtained from the methanolic reaction mixture were well-resolved; with *L*¹ only one solution species was present whilst with *L*², the signals were broadened and two solution species in a 5:1 ratio were observed. For the reasons discussed above for the copper(II) complexes, the sub-spectrum in the complexes with *L*² is assigned to a diastereomeric helicate with line broadening indicative of a fluxional structure; specifically, the chemical shifts and signal appearance do not resemble the mononuclear

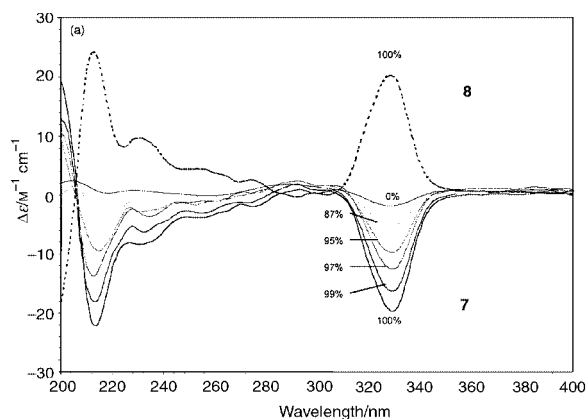


Fig. 7 Circular dichroism spectra of solutions of the enantiomeric complexes *M*-7 and *P*-8 in MeOH showing the loss of the CD response as MeCN is added to form the mononuclear species 3 and 4; in each case the concentration given is that of MeOH and the remainder is MeCN.

species observed in CD₃CN (see below). Samples of the complexes with L² recrystallised from MeNO₂ contained *only* the major solution species and *did not* regenerate the minor compound within hours, paralleling the behaviour of the analogous copper(i) complexes.

If the above interpretation is correct, the 6-methyl substituent in [Ag₂(L²)₂][PF₆]₂ affects the diastereoselectivity of helicate formation. Whereas the L¹ complexes give only one solution species in weak donor solvents (DE = 100%), L² gives a DE of 68%. Although NMR spectroscopy cannot distinguish between *HT* and *HH* isomers, modelling again suggests that *HT* helicates will be favored. This would also suggest that the additional interactions between the methyl and bornyloxy substituents of different helicands destabilise the system and lower the diastereoselectivity.

Solutions of the crude complexes with L¹ and L² in CD₃CN exhibited in all cases only one solution species and were well-resolved. Some of the resonances, particularly within the substituent, showed significant variation with respect to solutions in CD₃OD ($\Delta\delta \approx 0.75$). Crystals obtained from MeNO₂ or MeCN dissolved in CD₃CN gave identical spectra to those of the crude materials. ¹H NMR spectra of solutions varying in composition from pure CD₃OD to pure CD₃CN revealed solvent-dependent and reversible changes. In the less coordinating CD₃OD solvent, spectra of the type previously tentatively assigned to solution double-helical species were observed.³⁵ A key resonance is that of H^{6C} in L¹: it is found at δ 8.39 in CD₃CN but at δ 7.87 in CD₃OD. The upfield shift is not simply a medium effect, as all other aromatic resonances vary by less than δ 0.1, but is consistent with the presence of [AgL(MeCN)]⁺ in MeCN and double-helical [Ag₂(L₂)₂]²⁺ in CD₃OD: in the latter, H^{6C} is shielded by the second, adjacent helicand. The 6-methyl resonance in the complexes of L² is broadened in CD₃OD ($\Delta\nu_{1/2} \leq 20$ Hz) but not CD₃CN ($\Delta\nu_{1/2} \leq 2$ Hz) and H^{5endo}, H^{6endo} and H^{6exo} shift upfield in CD₃OD, compatible with ring-current effects arising from a double-helical solution species. These results strongly suggest that dinuclear species are present in non-coordinating solvents (MeOH and MeNO₂). In CD₃OD/CD₃CN solutions of [Ag₂(L¹)₂][PF₆]₂ containing 40% CD₃CN or [Ag₂(L²)₂][PF₆]₂ containing 20–35% CD₃CN, all signals are significantly broadened. Attempts to quantify the interconversion process by variable temperature experiments were unsuccessful. In contrast to the isolated solids discussed above, the evidence for mononuclear complexes 3–6 with both L¹ and L² in MeCN solution is overwhelming.

Chiroptical properties. The CD spectra of MeOH solutions of complexes with L¹ recrystallised from MeNO₂ are presented in Fig. 7; the responses are equal and opposite for the two

complexes and very similar results are obtained for the complexes with L². The CD response is low in comparison to qtpy helicates but significantly higher than that of the copper(i) complexes above and also than those reported for a related, helical silver(i) compound⁵⁰ or toroidal, hexanuclear silver(i) complexes.²⁰ The same crystals dissolved in MeCN display only very weak activity, ($\Delta\epsilon_{\text{max}} \leq \pm 2 \text{ M}^{-1} \text{ cm}^{-1}$) comparable to that of the free ligands. As the ¹H NMR studies showed that interconversion of diastereomeric helicates is slow, the differences in CD₃CN and CD₃OD solution must be due to mono- and dinuclear solution species. The CD responses in MeOH are 10 to 20 times larger than in MeCN, compatible with a diastereomeric excess of *P* or *M* double helicate in the former.¹³

The addition of MeCN to solutions of the complexes in MeOH reduced the CD activity (Fig. 7) compatible with the conversion of double helicates 7–10 to the less active mononuclear complexes 3–6. The MeCN concentration required to induce significant changes in the CD curves (5–30%) were somewhat lower than required in the NMR experiments, presumably because the complex concentrations in the former experiments were ≈ 100 times lower ($c \approx 2.5 \times 10^{-4} \text{ M}$).

The optical activity is also diagnostic. In MeCN, molar rotations of ± 620 – 640° are observed, typical of mononuclear complexes in which the main contribution is from the ligand chirality (± 220 – 250°). In contrast, much higher values ($\pm 1,500$ – $2,500^\circ$) are observed in MeOH indicative of the additional contribution of the double helix.¹³ Solutions of 7 in Me₂CO, CH₂Cl₂ or MeNO₂ all exhibited molar optical rotations in the range of $-2,500$ – $3,000^\circ$ indicating that the double helix persists in these solvents.

The preferred solution helicity of the complexes is indicated by the absolute sign of the 330 nm CD band and suggests formulations *M*-7, *P*-8, *M*-9 and *P*-10, assignments that parallel those of the copper(i) complexes with the same ligands.

For the first time we have been able to study the interconversion of double helicates and mononuclear complexes in solution. Taken together, the NMR and CD results explicitly confirm the presence of a double-helical species in non-coordinating solvents and show that the helical architecture, and not the ligand chirality, govern the appearance and magnitude of CD spectra.

Solid state structures of silver complexes. The data discussed above suggested that both mononuclear and dinuclear silver solution species could be formed, although the solid state IR data were somewhat ambiguous. Furthermore, although the CD spectra indicated whether *P* or *M* helical chirality was favored, we wished to confirm this and to establish whether *HH* or *HT* directional selectivity was observed.

3-Et₂O.³² Crystals of this complex were obtained by the diffusion of diethyl ether vapor into an MeCN solution of the crude product obtained from reaction with **I**. The asymmetric unit consists of two very similar [Ag(I)(MeCN)]⁺ cations (Fig. 8a). The silver is four-coordinate and in an N₄ environment generated by the three nitrogen donors of **I** and an MeCN molecule; the cation is essentially planar, with the sum of angles around the silver centres amounting to $360 \pm 1^\circ$. The bond angles and distances are within the range of other [Ag(Xterpy)(MeCN)]⁺ cations³⁵ and do not significantly differ in the two cations of the asymmetric unit. The Ag–NCMe distances are unremarkable (2.231(4) and 2.237(4) Å) but the contacts to **I** are all different and increase from the unsubstituted pyridine ring (2.318(3), 2.318(3) Å) over the central pyridine (2.403(3), 2.418(3) Å) to the bornyloxy-substituted pyridine (2.483(3), 2.480(3) Å). The longer Ag–N distance to the terminal bornyloxy substituted pyridines also slightly reduces the bite angle (66 – 67° versus 68 – 69°). The silver lies 0.13 – 0.15 Å out of the plane defined by the three terpy nitrogen atoms and the MeCN lies 0.51 – 0.66 Å above this plane. The cations are stacked in the lattice with a zigzag arrangement of silver centers (Ag...Ag 5.277, 5.577 Å,

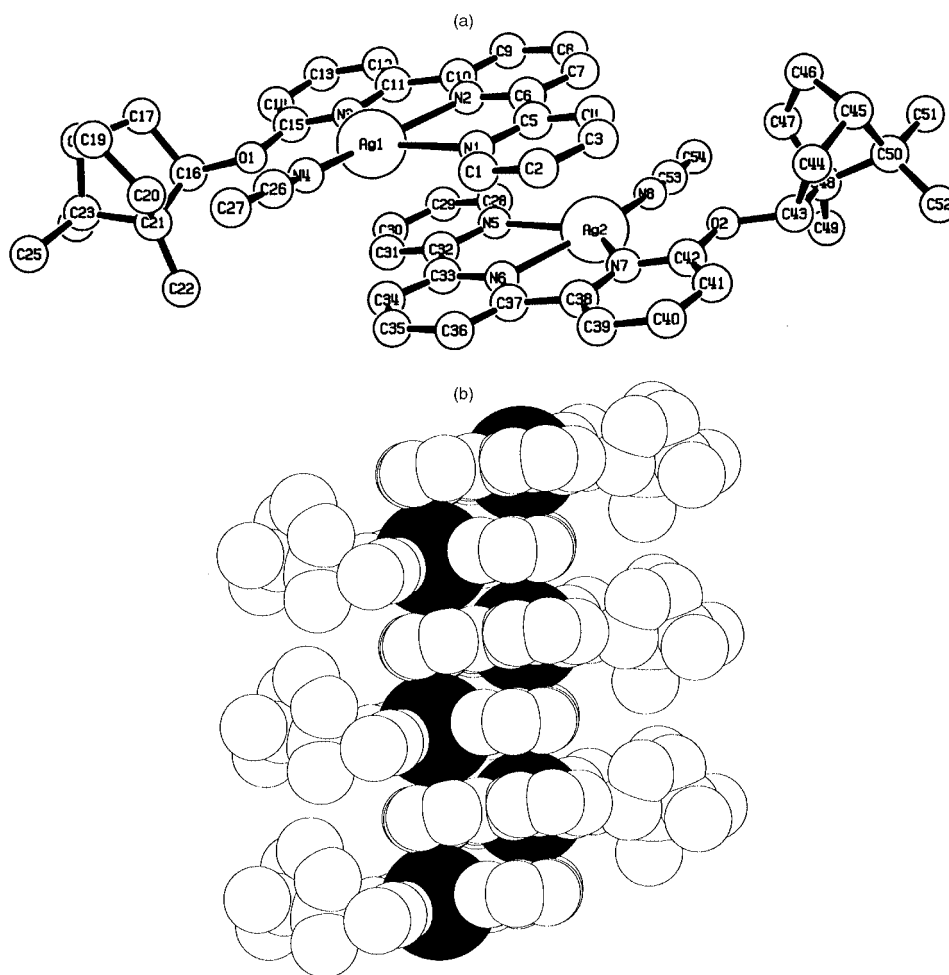


Fig. 8 Crystal and molecular structure of (a) the crystallographically independent pair of mononuclear cations in the lattice of $3 \cdot \text{Et}_2\text{O}$ showing the numbering scheme; H atoms omitted for clarity and (b) a space-filling representation of the packing in the lattice showing the zigzag arrangement of the π -stacked cations.

$\text{Ag}(1) - \text{Ag}(2) - \text{Ag}(1')$ 47.4°) resulting in efficient sandwiching of the silver centres between aromatic rings ($\text{Ag} \cdots \pi$ centroid distances: 3.646, 3.514 Å) and extensive interligand $\pi - \pi$ interactions (Fig. 8b). The stacked terminal pyridine rings are slightly offset with respect to each other, whilst the central pyridine sits directly above the silver(i) center of the adjacent molecule and *vice versa*. In the $[\text{Ag}(\text{terpy})(\text{MeCN})]^+$ cation, discrete dimeric units are observed with the two MeCN ligands twisted by 137.27° with respect to each other,³⁵ whereas in the cation of **3** they are oriented in opposite directions. The globular substituents point outwards and do not interfere with stacking interactions, which appear to significantly stabilise this solvato species in the solid state.

7·MeCOMe.³² This complex was obtained as an acetone solvate by the diffusion of Et_2O vapor into an MeCOMe solution of the complex initially recrystallised from MeNO_2 . The structural determination confirmed that double-helical dinuclear cations were present although considerable disorder existed in the lattice solvent molecules and the hexafluorophosphate anions. However, the structure was rather more complex than originally anticipated. The individual double-helical cations associate through short $\text{Ag} \cdots \text{Ag}$ interactions to form a tetranuclear $[\{\text{Ag}_2(\text{I})_2\}_2]^{4+}$ cation in the solid state. Within each tetranuclear subunit, one of the chiral substituents is disordered. Both of the dinuclear subunits exhibit an *HH*-conformation. However, the structure held additional surprises. There are two crystallographically independent tetranuclear cations in the asymmetric unit; in one, both of the dinuclear subunits possess *P*-helicity whilst in the other they are *M*-helicates. In the solid state, a *pseudo racemate* has formed

with a DE of 0%. We use the term *pseudo racemate* to indicate the mixtures containing equal amounts of the pairs of diastereomers $\{P\text{-(S;S)} + M\text{-(S;S)}\}$ or $\{P\text{-(R;R)} + M\text{-(R;R)}\}$. This illustrates the danger of relying on solid state data in isolation; the solution studies discussed above are *only* consistent with the presence of significant diastereomeric excesses of *M*-**7** and *P*-**8** helicates. The packing effects in the *pseudo racemate* appear to be sufficient to stabilise this structure in the solid state. It has been proposed that racemates containing centres of symmetry, planes of symmetry, or glide planes, show closer packing than enantiomerically pure solids⁵¹ and this appears to be the case with this complex. The molecular structure of the $[\{M\text{-Ag}_2(\text{I})_2\}_2]^{4+}$ cation is presented in Fig. 9a.

Although the two $[\{\text{Ag}_2(\text{I})_2\}_2]^{4+}$ cations differ in their helical chirality, bond lengths and angles are very similar in both structures although the individual $[\text{Ag}_2(\text{I})_2]^{2+}$ cations within a tetranuclear assembly vary slightly. All of the silver centers are two-coordinate ($\text{N} - \text{Ag} - \text{N}$ $176.1 - 178.9^\circ$) with $\text{Ag} - \text{N}$ distances in the range 2.146–2.206 Å. There are no significant differences in $\text{Ag} - \text{N}$ bond lengths to the terminal rings of each ligand, but the long $\text{Ag} \cdots \text{N}$ contacts to the central pyridine ring are notable (2.562–2.632 Å). The $\text{Ag} \cdots \text{Ag}$ distances within each dinuclear subunit vary in the range 2.914–2.941 Å. Within each tetranuclear unit, the dimers form interhelical $\text{Ag} \cdots \text{Ag}$ contacts in the range 3.107–3.156 Å. If the bornyloxy substituents define the head of the ligand, the $\text{Ag} \cdots \text{Ag}$ contact between the two dimeric subunits is tail-to-tail. A head-to-head contact would not be possible due to steric interactions between the bornyloxy substituents. The tetranuclear subunits are almost linear with $\text{Ag} \cdots \text{Ag} \cdots \text{Ag} \cdots \text{Ag}$ angles of $174.3 - 175.3^\circ$, partly as a

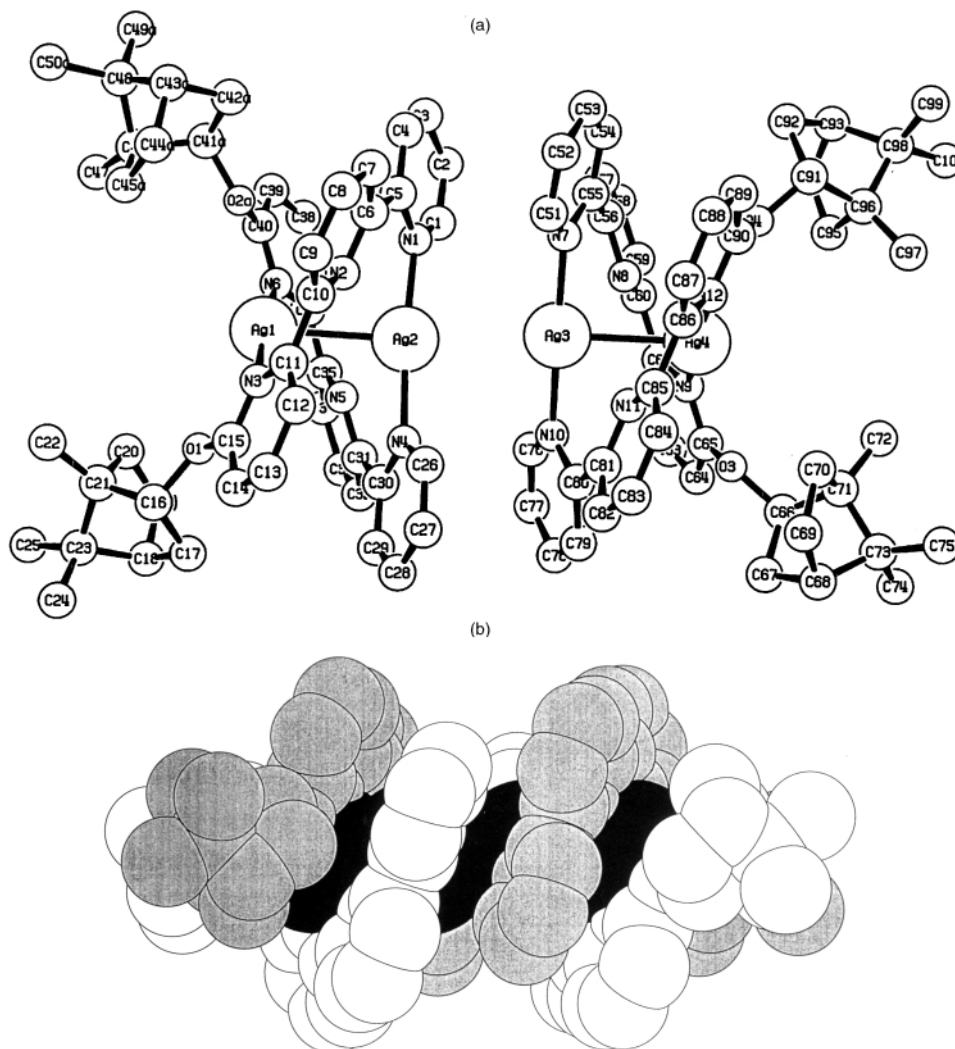


Fig. 9 Crystal and molecular structure of (a) the tetranuclear assembly of two *HH* double-helical cations in the lattice of 7-MeCOMe showing the numbering scheme; H atoms omitted for clarity as has the minor occupancy of the single disordered bornyloxy substituent; only the homochiral *MM* tetranuclear unit is shown (the symmetry related *PP* tetracation is present in the lattice in equal amounts), and (b) a space-filling representation emphasising the *MM*-helicity of the chosen tetranuclear unit.

result of the short $\text{Ag} \cdots \text{Ag}$ contact, significant interstrand and intrastrand π - π interactions occur between and within the cations of which the interligand interactions between the “tail” terminal pyridines in the range 3.669–3.783 Å are particularly significant (Fig. 9b).

The absence of diastereoselectivity in the solid state lead us to reinvestigate the solution properties of the crystals grown for the X-ray diffraction experiment. When one of these crystals was dissolved in CD_3OD , a ^1H NMR spectrum identical to that of the crude material was obtained, with only one solution species. In order to rule out accidental shift coincidence of diastereomeric *P*- and *M*-helicates, aliquots of the chiral shift reagent $[\text{Eu}(\text{tfc})_3]$ [$\text{tfc} = 3$ -(trifluoromethylhydroxymethylene)-(\mp)-camphorate] was added to a CD_2Cl_2 solution of the crystals in increasing amounts. No signal splitting was observed at the highest concentration of shift reagent. This result leads us to the conclusion that, in contrast to the solid state, only one solution species, *M*-7 (from CD spectroscopy), exists. A similar observation has been reported for mononuclear complexes⁵² and it appears to be a consequence of a low energy barrier for the interconversion of the diastereomers combined with crystal packing effects of the same order as the energy difference between the diastereomers. Although it is tempting to suggest that the solution species is the *HH* directional isomer observed in the solid state, there is no direct evidence to suggest this.

$[\text{Ag}_2(\text{L}^2)_2][\text{PF}_6]_2$. As noted above, we were aware that, although L^2 complexes were mononuclear in MeCN solution,

the solid state species obtained from MeCN exhibited no nitrile stretches in their IR spectra. Recrystallisation of the complex with **IV** from MeNO_2 gave the expected dinuclear double-helical complex **10**. However, recrystallisation of the complex with **III** from solutions in MeCN which unequivocally (CD, NMR) contained only mononuclear **5** also gave a dinuclear double helicate, **9**. Despite the different growth conditions, the two enantiomeric helicates **9** and **10** displayed identical unit cell parameters and structural features vary only within experimental error. Only the complex **10** will be discussed. In each case, single diastereomers of *HT*-isomers are found in the solid state, in contrast to the *HH* isomers found with L^1 . The cation in **9** showed *M* helical chirality whilst that in **10** adopted a *P* conformation. The structure of the cation in *P*-**10** is presented in Fig. 10.

The gross structural features of the cations closely resemble those of **1** and **2** with differences being primarily due to the ionic radius of silver(I) being larger than that of copper(I). The helical pitch depends on the intermetallic separation and the $\text{Ag} \cdots \text{Ag}$ distances (2.9387(10) and 2.9321(9) Å) are considerably longer than in **1** and **2**. The two silver centres within the double helicate are identical and best described as two-coordinate ($\text{N}-\text{Ag}-\text{N}$, *ca.* 172°; $\text{Ag}-\text{N}$, 2.153–2.165 Å) and the general structure resembles the dinuclear subunits observed in **7**. Longer contacts to the central pyridine rings are also present ($\text{Ag} \cdots \text{N}$, 2.616(2) Å, 2.630(3) Å). The helical twist is a result of successive interannular torsions between the

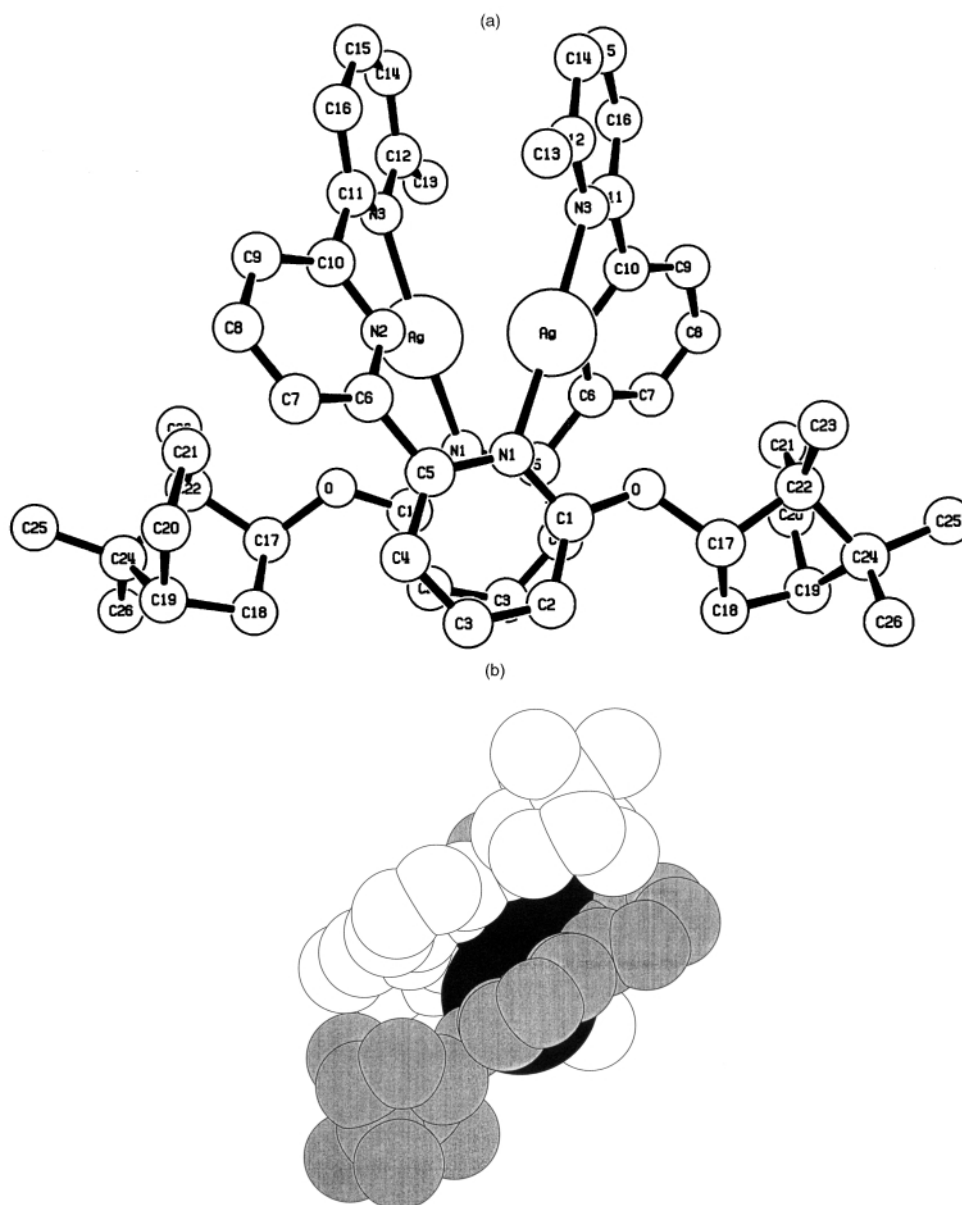


Fig. 10 Crystal and molecular structure of (a) the *HT* double-helical cation in the lattice of *P*-10 showing the numbering scheme; H atoms omitted for clarity and (b) a space-filling representation emphasising the *P*-helicity and showing the intramolecular π -stacking.

individual pyridine rings (26.3° , 36.9°) and the double-helical assembly is further stabilised by efficient π -stacking interactions between the 6-methyl-substituted pyridines (average interplanar distance 3.63 \AA).

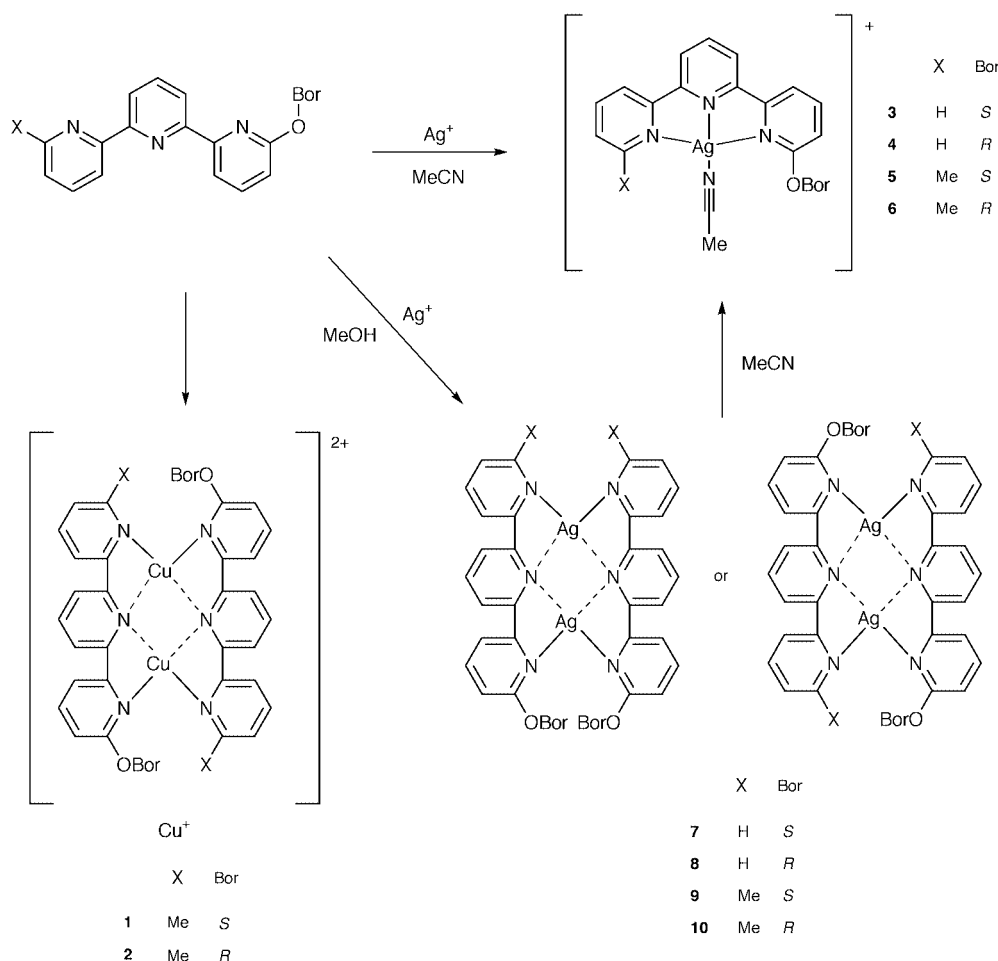
Helicates derived from L^2 cannot form tetranuclear assemblies, since efficient interhelical π -stacking or $\text{Ag} \cdots \text{Ag}$ interactions are not possible in either *HH* or *HT* isomers. In each case, interactions between the substituents prevent close approach. Minimised steric interactions between the chiral substituents favor the *HT* rather than *HH* isomers. However, the diastereoselectivity for *P* or *M* helical chirality is reduced because in both cases, there will be unfavorable interactions between the substituents. This appears to be the real role of the methyl substituents in giving diminished diastereoselectivity and the origin of the 68% DE with L^2 .

The influence of the 6-methyl substituents also controls the equilibration between mononuclear and dinuclear species in the solid state. The lattice containing $[\text{Ag}(L^1)(\text{MeCN})]^+$ cations is stabilised in the solid state by intermolecular $\text{Ag}-\pi$ and π -stacking interactions. The incorporation of the 6-methyl substituent would reduce these effects in $[\text{Ag}(L^2)(\text{MeCN})]^+$ (as seen in the solid state structure of **III**) offering an explanation for the

formation of the $[\text{Ag}_2(L^2)_2][\text{PF}_6]_2$ solid state species from solutions containing $[\text{Ag}(L^2)(\text{MeCN})]^+$. Modelling indicates that the 6-methyl substituents significantly restrict the site available for MeCN coordination; a similar observation has been made for $[\text{Ag}(L)(\text{MeCN})]^+$ ($L = 6,6''$ -diphenyl-2,2':6',2''-terpyridine) where the phenyl substituents twist to provide a pocket for the MeCN with the consequence that stacking and $\text{Ag} \cdots \text{Ag}$ interactions are reduced.³⁵ The summation of observations obtained by solid-state, IR-, CD- and NMR-spectroscopic analysis all generate the same impression: silver terpy dinuclear double-helicates are reasonably robust species. All of these transformations are summarised in Scheme 2.

Conclusion

We have demonstrated the synthesis of disilver(I) and dicopper(I) double helicates with chiral terpy ligands. Aryl substituents are not needed to stabilise dicopper(I) terpy helicates. The summation of observations obtained by solid-state structural, IR, CD and ^1H NMR spectroscopic analysis all generate the same impression: silver terpy helicates are not that fragile. The helicates were obtained regioselectively and with partial or



Scheme 2

complete diastereoselectivity. The interconversion of mononuclear and dinuclear double-helical silver complexes in solution was established by ^1H NMR and CD spectroscopy. CD titrations unequivocally allowed this interconversion to be studied and represent the first systematic study of the reversible interconversion of mononuclear complexes and double helicates with chiral ligands. The CD titrations provide compelling evidence that the helix and not the chiral ligand is the main contributor to measurable chiroptical effects in double helicates. 'Innocent' methyl substituents have profound effects in the solid state, but do not significantly affect the solution properties.

Experimental

General

The IR spectra were recorded on a Mattson Genesis FT spectrophotometer with samples in compressed KBr discs, ^1H NMR spectra on Bruker AM 250 or Avance 600 spectrometers, UV/Vis measurements using a Perkin-Elmer Lambda 19 spectrophotometer, TOF (Matrix Assisted Laser Desorption Ionisation) using a PerSeptive Biosystems Voyager-RP Biospectrometry Workstation, optical rotations using a Perkin-Elmer 141 polarimeter at the Na-D line using 10 cm quartz cuvettes and CD spectra on a Jasco J-720 CD spectrometer in 1 mm quartz cuvettes at 25 °C. The compounds 6-bromo-2,2':6',2''-terpyridine **V**,⁴² 2-acetyl-6-methylpyridine **VII**,^{43,44} 2-acetyl-6-bromopyridine⁴⁵ and 2-bromo-6-(3'-dimethylammonio-1'-oxopropyl)pyridine chloride **IX**^{46,47} were prepared following published procedures. The chiral compounds [(1*S*)-endo]-(-)- and [(1*R*)-endo]-(+)-borneol of best available enantiomeric purity were used as supplied by Aldrich.

Preparations

6-[(1*S*)-endo]-(-)-Borneyloxy-2,2':6',2''-terpyridine **I.** [(1*S*)-endo]-(-)-Borneol (0.616 g, 4 mmol) was added to a suspension of NaH (0.15 g, 60% dispersion in mineral oil, 4 mmol) in dry dmf (5 cm³) and the mixture heated to 80 °C. When hydrogen evolution had ceased, **V** (0.625 g, 2 mmol) was added and the solution turned green. Heating and stirring were continued for 16 h after which the reaction mixture was cooled and the solvent removed *in vacuo*. The remaining solid was partitioned between CH₂Cl₂ (50 cm³) and aqueous hydrochloric acid (2 M, 2 × 50 cm³). The aqueous phase was separated, neutralised with aqueous sodium hydroxide and the precipitate extracted with CH₂Cl₂ (2 × 20 cm³). The solvent was removed from the organic phase and the crude product purified by column chromatography (SiO₂, CH₂Cl₂-MeOH-0.880 NH₃ 90:9:1) with **I** eluting first. Recrystallisation from MeOH gave white crystals of **I** (0.55 g, 71%) mp 151–153 °C (Found: C, 77.9; H, 7.1; N 10.8. C₂₅H₂₇N₃O requires C, 77.9; H, 7.1; N, 10.9%); δ_{C} (CDCl₃) 13.85, 19.15, 19.81, 27.73, 28.16, 37.35, 45.04, 47.65, 48.98, 80.84, 111.76, 113.23, 120.59, 120.68, 121.16, 123.63, 136.79, 137.69, 138.99, 149.05, 153.46, 155.16, 155.47, 156.34, 163.86; $\tilde{\nu}_{\text{max}}/\text{cm}^{-1}$ 2945s, 1567s, 1439m, 1433s, 1252m, 775s (KBr); m/z 385 (M⁺), 248 (M - C₁₀H₁₇); $\lambda_{\text{max}}/\text{nm}$ (CHCl₃) 249 ($\epsilon/\text{M}^{-1}\text{cm}^{-1}$ 20.6 × 10³), 309 (23.3 × 10³).

6-[(1*R*)-endo]-(+)-Borneyloxy-2,2':6',2''-terpyridine **II.** As for **I** from **V** and [(1*R*)-endo]-(+)-borneol as white crystals (0.58 g, 75%) mp 151–153 °C (Found: C, 77.8; H, 7.2; N 10.9. C₂₅H₂₇N₃O requires C, 77.9; H, 7.1; N, 10.9%); ^{13}C NMR, MS and IR identical to **I**; UV/Vis (CHCl₃, 2.42 × 10⁻⁴ M): $\lambda_{\text{max}}/\text{nm}$ (CHCl₃) 249 nm ($\epsilon/\text{M}^{-1}\text{cm}^{-1}$ 21.1 × 10³), 309 (23.7 × 10³).

6-Bromo-6''-methyl-2,2':6',2''-terpyridine VI. A mixture of 2-acetyl-6-methylpyridine (1.22 g, 9.0 mmol) and iodine (2.29 g, 9.0 mmol) in pyridine (8 cm³) was heated to reflux for 1 h. The reaction mixture was then cooled, the solvent removed *in vacuo* and the residual yellow solid obtained washed well with diethyl ether and dried *in vacuo*. The yellow solid was obtained in 96% yield and consisted of a 1:1 mixture of pyridinium iodide and 2-[2-(6-methyl-2-pyridyl)-1-oxoethyl]pyridinium iodide **VIII** which was used without further purification. The 1:1 mixture (4.70 g, 8.6 mmol of **VIII**), **IX** (2.52 g, 8.6 mmol) and ammonium acetate (3.85 g, 50 mmol) were refluxed for 2 h in dry EtOH (25 cm³) after which the reaction mixture was cooled and the resulting precipitate collected and thoroughly washed with MeOH to leave silvery white, analytically pure flakes of **VI** (1.54 g, 55%) mp 215–217 °C (Found: C, 58.9; H, 3.8; N, 13.1; Br, 24.3. C₁₆H₁₂N₃Br requires C, 58.9; H, 3.7; N, 12.9; Br, 24.5%); δ_{C} (CDCl₃) 25.19, 118.63, 120.34, 121.75, 122.18, 123.91, 128.45, 137.52, 138.42, 139.64, 142.10, 154.20, 155.98, 156.39, 158.13, 158.51; $\tilde{\nu}_{\text{max}}/\text{cm}^{-1}$ 1571s, 1549s, 783s; MS (MALDI, TOF): m/z 325/7 (M)⁺, 246 (M – Br).

6-[(1S)-endo]-(-)-Boryloxy-6''-methyl-2,2':6',2''-terpyridine III. As for **I** substituting **VI** (0.65 g, 2 mmol) for **V**. After recrystallisation from MeOH, white crystals of **III** were obtained (0.41 g, 52%) mp 177–179 °C (Found: C, 78.0; H, 7.3; N, 10.5. C₂₆H₂₉N₃O requires C, 78.1; H, 7.3; N, 10.5%); δ_{C} (CDCl₃) 13.85, 19.16, 19.83, 24.65, 27.16, 28.18, 37.37, 45.08, 47.66, 48.99, 80.81, 111.69, 113.26, 118.14, 120.49, 120.66, 123.17, 136.93, 137.58, 138.98, 153.59, 155.41, 155.49, 155.76, 157.76, 163.85; $\tilde{\nu}_{\text{max}}/\text{cm}^{-1}$ 2956m, 1571s, 1434m, 1433s, 1262m, 787m; m/z 399 (M)⁺, 262 (M – C₁₀H₁₇); $\lambda_{\text{max}}/\text{nm}$ (CHCl₃) 250 ($\epsilon/\text{dm}^3 \text{ mol}^{-1} \text{ cm}^{-1}$ 18.3 × 10³), 309 (23.4 × 10³).

6-[(1R)-endo]-(+)-Boryloxy-6''-methyl-2,2':6',2''-terpyridine IV. As for **II** substituting **VI** (0.65g, 2 mmol) for **V**. After recrystallisation from MeOH, white crystals of **IV** were obtained (0.40 g, 50%) mp 178–179 °C (Found: C, 77.6; H, 7.1; N, 10.3. C₂₆H₂₉N₃O requires C, 78.1; H, 7.3; N, 10.5%); ¹³C NMR, MS and IR identical to **III**; $\lambda_{\text{max}}/\text{nm}$ (CHCl₃) 249 ($\epsilon/\text{dm}^3 \text{ mol}^{-1} \text{ cm}^{-1}$ 18.2 × 10³), 309 (23.3 × 10³).

6-Methyl-2,2':6',2''-terpyridine X. Compound **X** was obtained as the second fraction eluting from the column in the synthesis of **III** and **IV**. Recrystallisation from MeOH gave white crystals of **X** (≈30%) mp 106–107 °C (Found: C, 76.8; H, 5.3; N, 17.1. C₁₆H₁₃N₃ requires C, 77.1; H, 5.3; N, 17.0%); δ_{C} (CDCl₃) 24.16, 118.01, 120.72, 121.00, 121.13, 123.23, 123.63, 136.77, 136.30, 137.75, 149.02, 155.19, 155.56, 155.60, 155.23, 157.79; $\tilde{\nu}_{\text{max}}/\text{cm}^{-1}$ 2994w, 1560s, 1426s, 787m; m/z 263 (M)⁺.

General method for copper(I) complexes. [Cu(MeCN)₄][PF₆] (37.5 mg, 0.1 mmol) in degassed MeCN or MeOH (2 cm³) was treated with the appropriate ligand (0.1 mmol) under argon and the mixture ultrasonicated for 5–10 min to give orange-red solutions after which any remaining solid was removed by filtration over Celite and the solvent removed *in vacuo*. The complexes were recrystallised by slow diffusion of diethyl ether vapour into MeCN or MeOH solutions.

[Cu₂(**III**)₂][PF₆]₂ **1**. Orange crystals (44.0 mg, 72%) (Found: C, 51.5; H, 4.8; N, 7.2. C₅₂H₅₈F₁₂N₆O₂P₂Cu₂ requires C, 51.4; H, 4.8; N, 6.9%); $\tilde{\nu}_{\text{max}}/\text{cm}^{-1}$ 2966s, 2942m, 1604s, 1571s, 1475s, 1457s, 1030m, 841s, 557s; m/z 926 (M – 2PF₆), 790 (M – 2PF₆ – C₁₀H₁₇), 399 (**III**); $\lambda_{\text{max}}/\text{nm}$ (MeCN) 309 ($\epsilon/\text{dm}^3 \text{ mol}^{-1} \text{ cm}^{-1}$ 36.4 × 10³), 442 (1.58 × 10³).

[Cu₂(**IV**)₂][PF₆]₂ **2**. Orange crystals (47.0 mg, 78%) (Found: C, 51.6; H, 4.8; N, 7.0. C₅₂H₅₈F₁₂N₆O₂P₂Cu₂ requires C, 51.4; H, 4.8; N, 6.9%); IR, UV and MS as [Cu₂(**III**)₂][PF₆]₂.

General method for silver(I) complexes. A solution of AgOAc (8.3 mg, 0.05 mmol) in MeOH (5 cm³) was treated with the appropriate ligand (0.05 mmol) and the mixture ultrasonicated for 10 min at room temperature after which a clear solution had been obtained. After filtration over Celite, aqueous NH₄PF₆ was added and the precipitate filtered off, washed with water and dried (P₂O₅). Recrystallisation by diffusion of diethyl ether vapour into MeCN, MeOH or MeNO₂ solutions gave good quality crystals.

[Ag₂(**I**)₂][PF₆]₂ **7**. White crystals (32 mg, 100%) (Found: C, 47.0; H, 4.3; N, 6.7. C₅₀H₅₄F₁₂N₆O₂P₂Ag₂ requires C, 47.0; H, 4.3; N, 6.6%); $\tilde{\nu}_{\text{max}}/\text{cm}^{-1}$ 3195m, 2955s, 2878m, 1598s, 1575s, 1470s, 1456s, 1029m, 843s, 558s; m/z 1132.0 (M – PF₆), 878 (Ag(**I**)₂), 493 (Ag(**I**)); $\lambda_{\text{max}}/\text{nm}$ (Me₂CO) 272 ($\epsilon/\text{dm}^3 \text{ mol}^{-1} \text{ cm}^{-1}$ 16.0 × 10³), 317 (34.7 × 10³).

[Ag₂(**II**)₂][PF₆]₂ **8**. White crystals (32 mg, 100%) (Found: C, 47.0; H, 4.3; N, 6.7. C₅₀H₅₄F₁₂N₆O₂P₂Ag₂ requires C, 47.0; H, 4.3; N, 6.6%); IR, UV and MS as [Ag₂(**I**)₂][PF₆]₂.

[Ag(**I**)(MeCN)][PF₆] **3** and [Ag(**II**)(MeCN)][PF₆] **4**. White crystals from MeCN; $\tilde{\nu}_{\text{max}}/\text{cm}^{-1}$ 2953s, 2877m, 2305w, 2273w, 1576s, 1467s, 1440s, 1029m, 843s, 558s; m/z 1132 (M – PF₆), 877 (Ag(**L**)₂), 493.2 (Ag(**L**)); $\lambda_{\text{max}}/\text{nm}$ (MeCN) 230 ($\epsilon/\text{dm}^3 \text{ mol}^{-1} \text{ cm}^{-1}$ 20.2 × 10³), 309 (16.6 × 10³), 317 (16.6 × 10³).

[Ag₂(**III**)₂][PF₆]₂ **9**. White crystals (32 mg, 98%) (Found: C, 47.6; H, 4.4; N, 6.5. C₅₂H₅₈F₁₂N₆O₂P₂Ag₂ requires C, 47.9; H, 4.5; N, 6.4%); $\tilde{\nu}_{\text{max}}/\text{cm}^{-1}$ 2958s, 2880m, 1571s, 1470m, 1435s, 1263s, 1025m, 843s, 560s; m/z 1160 (M – PF₆), 906 (Ag(**III**)₂), 507 (Ag(**III**)); $\lambda_{\text{max}}/\text{nm}$ (Me₂CO) 279 ($\epsilon/\text{dm}^3 \text{ mol}^{-1} \text{ cm}^{-1}$ 18.7 × 10³), 318 (32.7 × 10³).

[Ag₂(**IV**)₂][PF₆]₂ **10**. White crystals (33 mg, 100%) (Found: C, 47.5; H, 4.4; N, 6.7. C₅₂H₅₈F₁₂N₆O₂P₂Ag₂ requires C, 47.9; H, 4.5; N, 6.4%); IR, UV and MS as [Ag₂(**III**)₂][PF₆]₂.

X-ray crystallography

Table 5 provides a summary of the crystal data, data collection, and refinement parameters for the new crystal structures reported in this paper. Data for the enantiomer **II** have been lodged with the CCDC but are not discussed in detail in this paper. The structures were solved by direct methods and refined using standard methods and techniques we have described previously^{13,36,37} using the programs SHELXS-86, SHELXL-93, SHELXL-97, SHELXS-97,⁵³ CRYSTALS⁵⁴ and SIR92.⁵⁵ For some structures a Chebychev weighting scheme⁵⁶ or DIFABS⁵⁷ were used. Crystallographic data (excluding structure factors) for the structures reported in this paper have been deposited with the Cambridge Crystallographic Data Centre and may be retrieved under Refcodes JOFPAV ([Ag(**I**)(MeCN)][PF₆].Et₂O,³² JOFQAW ([Ag₂(**I**)₂][PF₆]₂·Me₂CO),³² TURDEP ([Cu₂(**III**)₂][PF₆]₂·2MeCN),³¹ TURDIT ([Cu₂(**IV**)₂][PF₆]₂·2MeCN).³¹ CCDC reference number 186/1815.

See <http://www.rsc.org/suppdata/dt/a9/a909158k/> for crystallographic files in .cif format.

Acknowledgements

We thank the Schweizerischer Nationalfonds zur Förderung der wissenschaftlichen Forschung and the University of Basel for financial support of this work. We also thank Professors Alexander von Zelewsky and Jean-Pierre Sauvage for helpful discussions and provision of unpublished material.

References

- 1 R. W. Saalfrank and B. Demleitner, in *Transition Metals in Supramolecular Chemistry*, ed. J.-P. Sauvage, Wiley, Chichester, 1999, p. 1.
- 2 J.-C. Chambron, in *Transition Metals in Supramolecular Chemistry*, ed. J.-P. Sauvage, Wiley, Chichester, 1999, p. 225.
- 3 J.-C. Chambron, C. Dietrich-Buchecker and J.-P. Sauvage, in *Comprehensive Supramolecular Chemistry*, vol. 9, ed. J.-M. Lehn, Pergamon, Oxford, 1996, p. 85.

- 4 E. C. Constable, *Metals and Ligand Reactivity*, VCH, Weinheim, 1995.
- 5 E. C. Constable, *Tetrahedron*, 1992, **48**, 10013.
- 6 E. C. Constable, *Prog. Inorg. Chem.*, 1994, **42**, 67.
- 7 E. C. Constable, in *Comprehensive Supramolecular Chemistry*, ed. J.-M. Lehn, Pergamon, Oxford, 1996, vol. 9, p. 213.
- 8 C. Piguet, G. Bernardinelli and G. Hopfgartner, *Chem. Rev.*, 1997, **97**, 2005.
- 9 E. C. Constable, M. J. Hannon, P. Harverson, M. Neuburger, D. R. Smith, V. F. Wanner, L. A. Whall and M. Zehnder, *Polyhedron*, 2000, **19**, 23.
- 10 G. Baum, E. C. Constable, D. Fenske, C. E. Housecroft and T. Kulke, *Chem. Commun.*, 1999, 195.
- 11 E. C. Constable and J. V. Walker, *Polyhedron*, 1998, **17**, 3089.
- 12 E. C. Constable, F. R. Heitzler, M. Neuburger and M. Zehnder, *Chem. Commun.*, 1996, 933.
- 13 See G. Baum, E. C. Constable, D. Fenske, C. E. Housecroft and T. Kulke, *Chem. Eur. J.*, 1999, **5**, 1862 for further discussion of this point.
- 14 R. Krämer, J.-M. Lehn, A. DeCian and J. Fischer, *Angew. Chem., Int. Ed. Engl.*, 1993, **32**, 703.
- 15 P. N. Baxter, J.-M. Lehn and K. Rissanen, *Chem. Commun.*, 1997, 1323.
- 16 W. Zarges, J. Hall, J.-M. Lehn and C. Bolm, *Helv. Chim. Acta*, 1991, **74**, 1843.
- 17 C. R. Woods, M. Benaglia, F. Cozzi and J. S. Siegel, *Angew. Chem., Int. Ed. Engl.*, 1996, **35**, 1830.
- 18 A. L. Airey, G. F. Swiegers, A. C. Willis and S. B. Wild, *Inorg. Chem.*, 1997, **36**, 1588.
- 19 C. Provent, S. Hewage, G. Brand, G. Bernardinelli, L. J. Charbonniere and A. F. Williams, *Angew. Chem., Int. Ed. Engl.*, 1997, **36**, 1287.
- 20 O. Mamula, A. von Zelewsky and G. Bernardinelli, *Angew. Chem., Int. Ed.*, 1998, **37**, 289.
- 21 H. Mürner, G. Hopfgartner and A. von Zelewsky, *Inorg. Chim. Acta*, 1998, **271**, 36.
- 22 J. W. Canary, C. S. Allen, J. M. Castagnetto and Y. Wang, *J. Am. Chem. Soc.*, 1995, **115**, 8484.
- 23 C. R. Woods, M. Benaglia, P. Blom, A. Fuchicello, F. Cozzi and J. S. Siegel, *Polym. Prep.*, 1996, **37**, 480.
- 24 C. R. Woods, M. Benaglia, F. Cozzi and J. S. Siegel, *Angew. Chem., Int. Ed. Engl.*, 1996, **35**, 1830.
- 25 G. C. van Stein, G. van Koten and C. Brevard, *J. Organomet. Chem.*, 1982, **226**, 27.
- 26 G. C. van Stein, G. van Koten, B. de Bok, L. C. Taylor and K. Vrieze, *Inorg. Chim. Acta*, 1984, **89**, 29.
- 27 G. C. van Stein, G. van Koten, K. Vrieze, C. Brevard and A. L. Spek, *J. Am. Chem. Soc.*, 1984, **106**, 4486.
- 28 G. Baum, E. C. Constable, D. Fenske and T. Kulke, *Inorg. Chem. Commun.*, 1998, **1**, 80.
- 29 G. Baum, E. C. Constable, D. Fenske and T. Kulke, *Chem. Commun.*, 1997, 2043.
- 30 G. Baum, E. C. Constable, D. Fenske, C. E. Housecroft and T. Kulke, *Chem. Commun.*, 1999, 195.
- 31 E. C. Constable, T. Kulke, M. Neuburger and M. Zehnder, *Chem. Commun.*, 1997, 489.
- 32 G. Baum, E. C. Constable, D. Fenske, C. E. Housecroft and T. Kulke, *Chem. Commun.*, 1998, 2659.
- 33 E. C. Constable, A. J. Edwards, M. J. Hannon and P. R. Raithby, *J. Chem. Soc., Chem. Commun.*, 1994, 1991.
- 34 K. T. Potts, M. Keshavarz-K., F. S. Tham, H. D. Abruña and C. R. Arana, *Inorg. Chem.*, 1993, **32**, 4422.
- 35 E. C. Constable, A. J. Edwards, G. R. Haire, M. J. Hannon and P. R. Raithby, *Polyhedron*, 1998, **17**, 243.
- 36 E. C. Constable, T. Kulke, M. Neuburger and M. Zehnder, *New J. Chem.*, 1997, **21**, 633.
- 37 E. C. Constable, T. Kulke, M. Neuburger and M. Zehnder, *New J. Chem.*, 1997, **21**, 1091.
- 38 E. C. Constable, *Adv. Inorg. Chem. Radiochem.*, 1987, **30**, 69.
- 39 E. C. Constable, F. Heitzler, M. Neuburger and M. Zehnder, *J. Am. Chem. Soc.*, 1997, **119**, 5606.
- 40 E. C. Constable, F. R. Heitzler, M. Neuburger and M. Zehnder, *Supramol. Chem.*, 1995, **5**, 197.
- 41 E. C. Constable, F. R. Heitzler, M. Neuburger and M. Zehnder, *Chem. Commun.*, 1996, 933.
- 42 R. Chotalia, E. C. Constable, M. J. Hannon and D. A. Tocher, *J. Chem. Soc., Dalton Trans.*, 1995, 3571.
- 43 F. H. Case and T. J. Kasper, *J. Am. Chem. Soc.*, 1956, **78**, 5842.
- 44 H. B. Amin and R. Taylor, *J. Chem. Soc., Perkin Trans. 2*, 1979, 624.
- 45 F. Kröhnke, *Synthesis*, 1976, 1.
- 46 J. E. Parks, B. E. Wagner and R. H. Holm, *J. Organomet. Chem.*, 1973, **36**, 53.
- 47 E. C. Constable, J. M. Holmes and R. C. S. McQueen, *J. Chem. Soc., Dalton Trans.*, 1987, 5.
- 48 H. D. Flack, *Acta Crystallogr., Sect. A*, 1983, **39**, 876.
- 49 C. Provent, S. Hewage, G. Brand, G. Bernardinelli, L. J. Charbonniere and A. F. Williams, *Angew. Chem., Int. Ed. Engl.*, 1997, **36**, 1287.
- 50 M. Ziegler and A. von Zelewsky, *Coord. Chem. Rev.*, 1998, **177**, 257.
- 51 J. Jacques, A. Collet and S. H. Wilen, *Enantiomers, racemates and resolutions*, Wiley, Chichester, 1981, p. 81.
- 52 P. Biscarini, R. Franca and R. Kuroda, *Inorg. Chem.*, 1995, **34**, 4618.
- 53 G. M. Sheldrick, in *SHELX?*, Program for the solution of crystal structures, University of Göttingen, Germany, 1986–1997.
- 54 D. J. Watkin, J. R. Carruthers and P. Betteridge, *CRYSTALS*, Chemical Crystallography Laboratory, Oxford, UK, 1985.
- 55 A. Altomare, G. Cascarano, G. Giacovazzo, A. Guagliardi, M. C. Burla, G. Polidori and M. Camalli, *J. Appl. Cryst.*, 1994, **27**, 435.
- 56 J. R. Carruthers and D. J. Watkin, *Acta Crystallogr., Sect. A*, 1979, **35**, 698.
- 57 N. Walker and D. Stuart, *Acta Crystallogr., Sect. A*, 1983, **39**, 158.

Paper a909158k